NAVAL POSTGRADUATE SCHOOL
Monterey, California

AD-A283 418

DTIC
ELECTE
AUG 1 6 1994
S G D

THESIS

AN ANALYSIS OF A SINGLE-BURN ALGORITHM FOR LOW-
EARTH ORBIT MAINTENANCE

By

Paul A. Gardner

June 1994

Thesis Advisor: I.M. Ross

94-25702

94 8 15 075

REPORT DOCUMENT PAGE

Public reporting burden for this collection of information is estimated to average 1 hour per response, including the time for reviewing instructions, searching existing data sources, gathering and maintaining the data needed, and completing and reviewing the collection of information. Send comments regarding this burden estimate or any other aspect of this collection of information, including suggestions for reducing this burden, to Washington Headquarters Services, Directorate for Information Operations and Reports, 1215 Jefferson Davis Highway, suite 1204, Arlington, VA 22202 - 4302, and to the Office of Management and Budget, Paperwork Reduction Project (0704-0188), Washington, DC 20503

1. AGENCY USE ONLY (Leave Blank)	2. REPORT DATE	3. REPORT TYPE AND DATES COVERED
	16 JUNE 1994	Master's Thesis

4. TITLE AND SUBTITLE	5. FUNDING NUMBERS
AN ANALYSIS OF A SINGLE-BURN ALGORITHM FOR LOW-EARTH ORBIT MAINTENANCE	

6. AUTHORS

Gardner Paul A.

7. PERFORMING ORGANIZATION NAME(S) AND ADDRESS(ES)	8. PERFORMING ORGANIZATION REPORT NUMBER
Naval Postgraduate School Monterey, CA 93943-5000	

9. SPONSORING / MONITORING AGENCY NAME(S) AND ADDRESS(ES)	10. SPONSORING / MONITORING AGENCY REPORT NUMBER

11. SUPPLEMENTARY NOTES

The views expressed in this thesis are those of the author and do not reflect the official policy or position of the Department of Defense or the U. S. Government.

12a. DISTRIBUTION / AVAILABILITY STATEMENT	12b. DISTRIBUTION CODE
Approved for public release, distribution is unlimited.	A

13. ABSTRACT (MAXIMUM 200 WORDS)

With the requirement for a spacecraft to maintain an orbital altitude band, a simple energy balance algorithm has been developed using a combination of radial distance and spacecraft specific energy for fixed-vector thruster control. While each trajectory produces a unique band, initial attempts at producing a pre-specified band have been unsuccessful. It is theorized that a certain radial bandwidth would correspond to a specific set of control parameters, and that by creating maps of the relationship between the two for various spacecraft configurations a method of maintaining the pre-specified band could be found. This thesis studies variations in spacecraft configurations and finds dependence of orbital bandwidth on thrust-to-drag ratio and ballistic coefficient. Also, within certain ranges of control parameters, multiple trajectories produce equivalent radial bands. Analysis shows that all single-burn trajectories are characterized by similar efficiencies, and are less efficient than a Forced Keplerian Trajectory (FKT).

14. SUBJECT TERMS	15. NUMBER OF PAGES
Forced Keplerian Trajectory, thrust-to-drag ratio, ballistic coefficient, eccentricity, orbital decay, thruster cut-off energy	89
	16. PRICE CODE

17. SECURITY CLASSIFICATION OF REPORT	18. SECURITY CLASSIFICATION OF THIS PAGE	19. SECURITY CLASSIFICATION OF ABSTRACT	20. LIMITATION OF ABSTRACT
UNCLASSIFIED	UNCLASSIFIED	UNCLASSIFIED	UL

An Analysis of a Single-Burn Algorithm

for Low-Earth Orbit Maintenance

by

Paul A. Gardner
Lieutenant , United States Navy
B.S., United States Naval Academy, 1986

Submitted in partial fulfillment

of the requirements for the degree of

MASTER OF SCIENCE IN ASTRONAUTICAL ENGINEERING

from the

NAVAL POSTGRADUATE SCHOOL
June 16, 1994
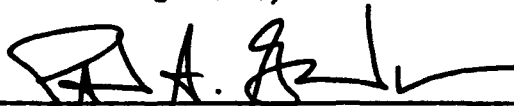
Author: _____
Paul A. Gardner

Approved by: _____
I. M. Ross, Thesis Advisor

_____
Sandi L. Scriyener, Second Reader .
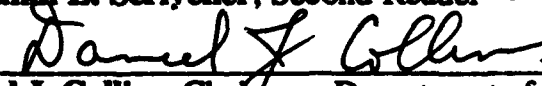
_____
Daniel J. Collins, Chairman, Department of
Aeronautics and Astronautics

ii

ABSTRACT

With the requirement for a spacecraft to maintain an orbital altitude band, a simple energy balance algorithm has been developed using a combination of radial distance and spacecraft specific energy for fixed-vector thruster control. While each trajectory produces a unique band, initial attempts at producing a pre-specified band have been unsuccessful. It is theorized that a certain radial bandwidth would correspond to a specific set of control parameters, and that by creating maps of the relationship between the two for various spacecraft configurations a method of maintaining the pre-specified band could be found. This thesis studies variations in spacecraft configurations and finds dependence of orbital bandwidth on thrust-to-drag ratio and ballistic coefficient. Also, within certain ranges of the control parameters, multiple trajectories produce equivalent radial bands. Analysis shows that all single-burn trajectories are characterized by similar efficiencies, and are less efficient than a Forced Keplerian Trajectory (FKT).

Accesion For		
NTIS CRA&I		☑
DTIC TAB		☑
Unannounced		☐
Justification		
By		
Distribution /		
Availability Codes		
Dist	Avail and / or Special	
A-1		

iii

TABLE OF CONTENTS

I. INTRODUCTION

Optimizing orbit maintenance trajectories for low-Earth orbiting (LEO) spacecraft is increasingly important as space agencies around the world strive to maintain orbiting programs with shrinking budgets. Conceptually, an orbit may be maintained using a Forced Keplerian Trajectory (FKT), where thrust is used to cancel drag. This would prevent orbital decay, maintaining a true Keplerian orbit. While this strategy is technically impractical due to limitations in thrust vectoring and thrust magnitude adjustments, it does provide a benchmark by which other strategies may be measured. While optimal control theory [Ref. 1], shows that an FKT is not the optimal solution to the orbit maintenance problem with respect to fuel, studies have yet to find a trajectory which is more fuel-efficient.

Historically, most orbit reboost strategies have been based on the Hohmann transfer, consisting of two thruster burns, where the first burn starts the spacecraft on an elliptical path to a higher altitude, and the second burn circularizes the spacecraft's orbit at the desired altitude. The Eccentricity Intercept Targeting and Guidance (EITAG) trajectory developed by Gottlieb [Ref. 2] notes variations of eccentricity, e, vs semi-major axis, a, and integrates backwards in time from the desired orbit. A two burn trajectory is developed which reboosts and circularizes the orbit while minimizing errors in achieving the target orbit.

A third orbit maintenance strategy proceeds from the notion that a spacecraft must be maintained within a specific radial band. A space station, for example, must be maintained within an altitude band that can be reached by various launch vehicles for servicing and manning requirements. A precise, circular orbit is not necessary. With this in mind, a single-burn trajectory, boosting the spacecraft as it nears the lower altitude boundary, then allowing

1

it to decay over time, would maintain the required band while reducing the number of required burns, and perhaps, the fuel required for orbit maintenance.

Pauls [Ref. 3] and Wilsey [Ref. 4] developed a computer model for such a strategy, using various parameter variations to optimize the trajectory. While their results show that a single-burn trajectory is less fuel-efficient than the FKT benchmark, further study is warranted. In addition, an accurate method of predicting the actual controlled radial band is desired.

By non-dimensionalizing the equations of motion, greater clarity and precision will be achieved when varying the control parameters. These results will be used to create maps of radius and energy which will allow better control of the spacecraft's radial band.

II. DEVELOPMENT OF THE ORBIT MAINTENANCE PROCEDURE

A. NON-OPTIMALITY OF A FORCED KEPLERIAN TRAJECTORY

While optimal control theory techniques show that a Forced Keplerian Trajectory
(FKT) is not optimal with respect to fuel [Ref. 1], significant insight into the problem can be
gained by looking into an extremely simplified version of the orbit maintenance problem
[Ref. 5]. If an FKT is optimal, the theory should lead to an optimal control history where
thrust is equal to drag.
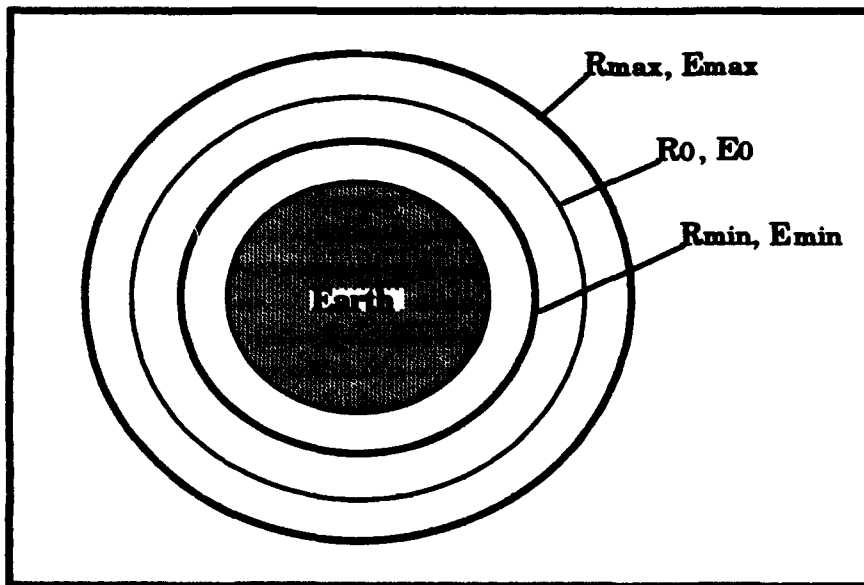
**Figure 1** Orbital band

The problem may be simplified by stating that the only requirement of the control system is
to maintain the orbit semi-major axis, a, and eccentricity, e, within such limits that the orbit
remains within the specified band. These two orbital elements define the shape of the orbit
within the orbital plane. This shape could theoretically vary from a circular orbit ($e=0$)

3

where a varies from R_{min} to R_{max} (see Figure 1), to an elliptical orbit with perigee equal to R_{min} and apogee equal to R_{max}, with e variation dependent upon the size of the band.

Further simplification is possible by looking only at the portion of the problem relating to semi-major axis, a. This leaves a one degree-of-freedom system for optimization. To get an equation of motion for semi-major axis, the work-energy theorem is used

$$\Delta E = \int F \cdot ds \qquad (1)$$

This can be used to relate the specific mechanical energy of the orbit to the forces involved, namely thrust and drag

$$\frac{d\varepsilon}{dt} = \left(\frac{T-D}{m} \right) \frac{ds}{dt}$$

$$= \left(\frac{T-D}{m} \right) v \qquad (2)$$

Recalling the definition of the specific mechanical energy, $\varepsilon = -\mu / 2a$,

$$\frac{d\varepsilon}{dt} = \frac{\mu}{2a^2} \frac{da}{dt} \qquad (3)$$

This leads to an equation for $\dot{a}$,

$$\dot{a} = \frac{2a^2 v}{\mu m} (T - D) \qquad (4)$$

The other equation of motion for the system comes from the rocket equation

$$\dot{m} = -\frac{T}{I_{sp} g_o} = -\frac{T}{v_e} \qquad (5)$$

4

where the specific impulse, I_{sp} and the acceleration due to gravity are multiplied to define the exhaust velocity of the engine, v_e.

The final major simplification comes from focusing on the band to be maintained. When attempting to maintain a small enough band, the change in a is small, so the squared term is essentially constant. Additionally, such a band would require a small change in velocity, Δv, to maintain it. Thus, v is also assumed to be constant. These assumptions allow Equation 4 to be rewritten as

$$\dot{a} = \frac{k}{m}(T-D) \tag{6}$$

where k is a constant.

The optimal control problem is now formulated as finding the control history that best transfers the spacecraft from some initial condition a_o to some final condition a_f. The optimality criterion is minimizing fuel burned, which can be stated as maximizing the final mass. The problem constraint is the available thrust, which is defined as

$$0 \le T \le T_{max} \tag{7}$$

Thrust is the single element of control in the simplified problem. From optimal control theory, the Hamiltonian is

$$H = \lambda_a \frac{k}{m}(T-D) - \lambda_m \frac{T}{v_e}$$

$$= \left(\frac{\lambda_a k}{m} - \frac{\lambda_m}{v_e} \right) T - \frac{\lambda_a kD}{m} \tag{8}$$

where λ_a and λ_m are the Lagrange multipliers, or costates of the system, corresponding to the semi-major axis and mass respectively.

Pontryagin's Maximum Principle (PMP) states that at every point on the trajectory of the system, the optimum control history maximizes the Hamiltonian. Stated mathematically,

$$u^* = \arg \max_{u \in U} H \qquad (9)$$

By examining Equation 8, it is clear that the control variable, T, that maximizes the H-function depends upon the sign to the quantity in brackets, which is called the switching function, s

$$s = \frac{\lambda_a k}{m} - \frac{\lambda_m}{v_e} \qquad (10)$$

Noting the constraint upon thrust, application of the PMP shows that

$$T = \begin{cases} T_{max} & s > 0 \\ 0 & s < 0 \end{cases} \qquad (11)$$

Called a bang-bang controller, this optimal control history contains no reference to drag; therefore the optimal control for such an orbital transfer does not define thrust equal to drag. The Forced Keplerian Trajectory is thus shown not be the optimal control method.

B. ORBIT CONTROL STRATEGY

It is desired to maintain a spacecraft within a specified radial band, using a single thruster firing to reboost the spacecraft when it nears the minimum radius. Wilsey [Ref. 4], shows that such a scheme is possible using radius and spacecraft specific energy as control parameters. Figure 1 shows such a radial band, defining radii and energies.

6

To facilitate this orbital control scheme, it is necessary to initiate thruster firing prior to the spacecraft decaying to the minimum altitude, and shut down thrusters prior to gaining the maximum altitude. Thruster firing is controlled by orbit radius, with

$$\delta r = R_0 - r_{th} \qquad (12)$$

where r_{th} is the radius of thruster initiation. Spacecraft specific energy is then monitored throughout the burn, with thruster cut-off occurring when

$$E = E_{th} \qquad (13)$$

with E_{th} being specific energy at thruster cut·off. By specifying values for δr and E_{th}, minimum and maximum radii will be achieved, denoted by r_{mn} and r_{mx}, respectively. This is pictured in Figure 2.
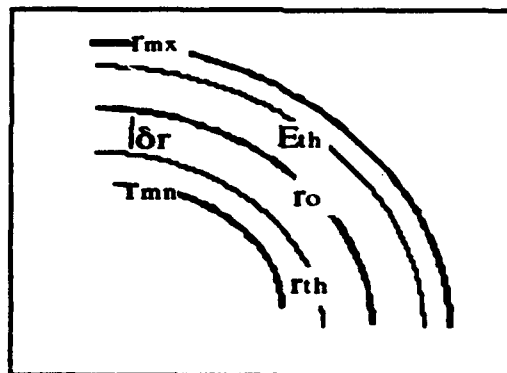
Figure 2 Thrust Control Parameters

The choices for δr and F_{th} will produce a unique maximum band, but what values correspond to the desired band? Does a specific, desired band produce a specific trajectory? How do the bands and associated trajectories vary with changes in spacecraft parameters such as thrust-to-drag ratio, specific impulse, and ballistic coefficient? Ross, Pauls, and Wilsey [Ref. 6] propose a simple "energy-balance" algorithm where δr and E_{th} are varied

7

until the desired radial band is achieved [Appendix. A]. By following this procedure and mapping δr and E_{th} as they vary with the actual band attained for different spacecraft configurations, a relationship between the parameters is sought which would remove the need for iteration and allow orbit trajectory prediction.

C. DEVELOPMENT OF THE EQUATIONS OF MOTION

The initial investigation of a single burn, low-earth orbit trajectory will be simplified by assuming an orbit which is initially circular. The spacecraft is a non-lifting (blunt) body, therefore the only aerodynamic force which affects it is drag. The external forces thus perturbing the orbit are aerodynamic drag, gravity, and thrust. Looking at the orbital dynamics as a two-body problem, the coordinate system may be defined as shown in Figure 3.
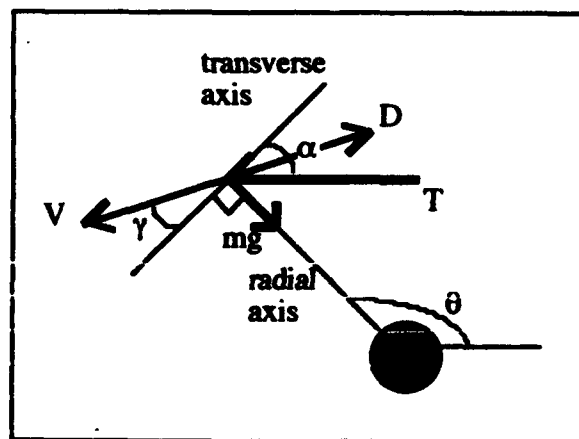

Figure 3 Orbital Coordinate System

The equations of motion for this system are

$$a_r = \sum \frac{F_r}{m} \tag{14}$$

8

$$a_{tr} = \sum \frac{F_{tr}}{m} \qquad (15)$$

where a_r and a_{tr} are the radial and transverse components of the inertial acceleration, ΣF_r and ΣF_{tr} are the sums of the respective forces, and m is the spacecraft mass. As seen in Figure 3, drag and thrust can each be broken into components

$$D_r = -D\sin(\gamma) \qquad D_{tr} = -D\cos(\gamma) \qquad (16a\&b)$$

$$T_r = T\sin(\alpha) \qquad T_{tr} = T\cos(\alpha) \qquad (17a\&b)$$

where γ denotes the flight path angle (between the velocity vector and the transverse axis), and α represents the thruster elevation angle (between the thrust vector and the transverse axis). Rewriting the equations of motion in polar coordinates using equations 16 and 17 leads to

$$\ddot{r} - \dot{\theta}^2 r = -\frac{\mu}{r^2} - \frac{D_r}{m} + \frac{T_r}{m} \qquad (18)$$

$$\ddot{\theta}r + 2\dot{\theta}\dot{r} = -\frac{D_{tr}}{m} + \frac{T_{tr}}{m} \qquad (19)$$

where μ is the earth's gravitational parameter, and θ is the angular position of the spacecraft.

D. NONDIMENSIONALIZATION OF THE EQUATIONS OF MOTION

When dealing with an orbital system, the use of standard dimensional units leads to large variations in numbers that cause computational errors. To counter this and to better study the effects of variation of certain parameters, a system of canonical units is developed to non-dimensionalize the equations of motion.

1. Definitions

To nondimensionalize the equations, base units for length, mass, and time are defined. The base length is the radius of the target orbit, which is defined as the midpoint of the desired radial band, and is denoted by r_b. The base mass is the initial spacecraft mass, and is denoted by m_b. The base time is defined as the period of a circular orbit at a radius of r_b divided by 2π, and is denoted by t_b,

$$t_b = \sqrt{\frac{r_b^3}{\mu}} \tag{20}$$

These base units are then used to define the nondimensionalized variables for radius, mass, and time

$$\overline{r} = \frac{r}{r_b} \tag{21}$$

$$\overline{m} = \frac{m}{m_b} \tag{22}$$

$$\overline{t} = \frac{t}{t_b} \tag{23}$$

The variable θ is dimensionless by definition.

In addition to the three "basic" units, a base unit for density is also defined, and denoted by ρ_b. Using a local exponential density model with atmospheric scale height β

$$\rho = \rho_o e^{-\beta(r-r_{ref})} \tag{24}$$

10

ρ_b is defined as equal to ρ_o. Nondimensionalizing β with r_b, and setting r_{ref} equal to r_b produces a nondimensionalized density

$$\bar{\rho} = e^{-\bar{\beta}(\bar{r}-1)} \tag{25a}$$

where

$$\bar{\beta} = \beta \, r_b \tag{25b}$$

This is used in the determination of drag, as drag is given by

$$D = \frac{1}{2}\rho A C_d v^2 \tag{26}$$

where A is the surface area, C_d the drag coefficient, and v the spacecraft velocity. A table of quantities, their nondimensionalized cousins and relating factors is given in Appendix B.

2. Equation Nondimensionalization

The above definitions are used to develop the nondimensionalized variable derivatives

$$\ddot{r} = \frac{d^2 r}{dt^2} = \frac{d}{dt}\left(\frac{dr}{dt}\right) = \frac{d}{dt}\left(\frac{d\bar{r}}{d\bar{t}}\right)\frac{r_b}{t_b} = \frac{d}{d\bar{t}\,t_b}\,(\bar{r}')\frac{r_b}{t_b} = \bar{r}''\frac{r_b}{t_b^2} \tag{27}$$

$$\ddot{\theta} = \frac{d^2\theta}{dt^2} = \frac{d}{dt}\left(\frac{d\theta}{dt}\right) = \frac{d}{dt}\left(\frac{d\theta}{d\bar{t}}\right)\frac{1}{t_b} = \frac{d}{d\bar{t}\,t_b}\,(\bar{\theta}')\frac{1}{t_b} = \bar{\theta}''\frac{1}{t_b^2} \tag{28}$$

where primes denote a nondimensionalized parameter differentiated with respect to time. These derivatives are used to yield the nondimensionalized equations of motion

$$\bar{r}'' = \bar{\theta}'^2 \bar{r} - \frac{1}{\bar{r}^2} - \frac{\bar{D}_r}{\bar{m}} + \frac{\bar{T}_r}{\bar{m}} \qquad (29)$$

$$\bar{\theta}'' \bar{r} + 2\bar{\theta}' \bar{r}' = -\frac{\bar{D}_\theta}{\bar{m}} + \frac{\bar{T}_\theta}{\bar{m}} \qquad (30)$$

where the nondimensionalized values of both drag and thrust components are related to their dimensionalized counterparts by the same factor

$$\bar{F} = F \frac{t_b^2}{m_b r_b} \ , F = D,T \qquad (31)$$

3. Parameter Development

To study the effects of varying spacecraft design parameters on the orbit trajectory and their related bands, nondimensionalized parameters are developed which represent ballistic coefficient, engine specific impulse, and thrust-to-drag ratio. These parameters can be thought of as quantifying atmospheric effects, spacecraft shape, and engine sizing.

a. Nondimensionalized Ballistic Coefficient, $\overline{B}$

Recalling equation 26, the nondimensionaliztion of drag requires the nondimensionalized density defined above, $\overline{\rho}$, and a nondimensionalized velocity, $\overline{v}$. Using the velocity equation

$$v^2 = \dot{r}^2 + r^2 \dot{\theta}^2 \qquad (32)$$

and the relationships in equations 27 and 28 gives

$$v^2 = \bar{v}^2 \frac{r_b^2}{t_b^2} \qquad (33)$$

12

which is substituted, along with $\overline{\rho}$ into equation 26. Nondimensionalizing drag using equation 31 gives

$$\overline{D} = \frac{1}{2} \overline{\rho} \, A C_d \, \overline{v}^2 \frac{\rho_b r_b}{m_b} \qquad (34)$$

By defining the ballistic coefficient as the base mass divided by the product of the surface area and the drag coefficient,

$$B = \frac{m_b}{A \, C_d} \qquad (35a)$$

the nondimensionalized ballistic coefficient is then defined as

$$\overline{B} = \frac{B}{\rho_b r_b} \qquad (35b)$$

which leads to the final nondimensionalized equation for drag

$$\overline{D} = \frac{1}{2} \frac{\overline{\rho} \, \overline{v}^2}{\overline{B}} \qquad (36)$$

b. Mass/Thrust Parameter, $\overline{p}$

Fuel mass flow and thrust are related by the rocket equation,

$$\dot{m} = - \frac{T}{I_{sp} g_o} \qquad (37)$$

Following the example of equation 27 when nondimensionalizing the derivative of mass and using the thrust relationship of equation 31, the nondimensionalized mass flow is written

13

$$\bar{m}' = -\bar{T}\frac{r_b}{I_{sp}g_o t_b} \tag{38}$$

By defining

$$\bar{p} = \frac{r_b}{I_{sp}g_o t_b} \tag{39}$$

variations in spacecraft specific impulse, I_{sp}, can be incorporated into a final

nondimensionalized equation for both mass flow and thrust

$$\bar{m}' = -\bar{p}\bar{T} \tag{40}$$

c. Thrust-to-Drag Ratio, $\bar{T}_D$

The thrust-to-drag ratio is defined as the thrust divided by the drag at the target

orbit. As both thrust and drag are forces and thus nondimensionalized by the same factors,

this ratio may be written

$$\bar{T}_D = \frac{\bar{T}}{\bar{D}_o} \tag{41}$$

III. COMPUTER MODEL DEVELOPMENT

A. ORIGINAL DEVELOPMENT

Originally developed by Pauls [Ref. 3] and refined by Wilsey [Ref. 4], a computer program, written in FORTRAN, was developed to simulate the orbital motion of a spacecraft. The main routine controlled input, output, and subroutine calls. Subroutines computed drag and orbital parameters, controlled thrust, and updated the equations of motion. A fourth-order Runge-Kutta numerical integration routine was used to integrate the equations of motion. The nondimensionalized equations were simplified by defining new state variables, which transformed the two second order differential equations into a set of four first order differentials.

B. STATE VARIABLE DEFINITIONS

A five element state vector, $\underline{x}$, is defined as

$$x_1 = r \tag{42}$$

$$x_2 = \dot{r} = \frac{dr}{dt} \tag{43}$$

$$x_3 = \theta \tag{44}$$

$$x_4 = \dot{\theta} = \frac{d\theta}{dt} \tag{45}$$

$$x_5 = m \tag{46}$$

15

These states can be nondimensionalized using the factors introduced previously and substituted into the equations of motion. Combining equations 29 and 30 with the nondimensionalized state variables produces

$$\frac{d\bar{x}_2}{d\bar{t}} = \bar{x}_1 \bar{x}_4^2 - \frac{1}{\bar{x}_1^2} - \frac{\bar{D}}{\bar{m}}\sin\gamma + \frac{\bar{T}}{\bar{m}}\sin\alpha \qquad (47)$$

$$\frac{d\bar{x}_4}{d\bar{t}} = -\frac{2\bar{x}_4 \bar{x}_2}{\bar{x}_1} - \frac{\bar{D}}{\bar{x}_1 \bar{m}}\cos\gamma + \frac{\bar{T}}{\bar{x}_1 \bar{m}}\cos\alpha \qquad (48)$$

As the flight path angle, γ, is a function of the velocity vector, the geometric functions can be represented by

$$\sin\gamma = \frac{\bar{x}_2}{\bar{v}} \qquad \cos\gamma = \frac{\bar{x}_1 \bar{x}_4}{\bar{v}} \qquad (49a\&b)$$

Substituting these relationships into equations 47 and 48 leads to the final equations of motion as they are programmed into the simulation:

$$\frac{d\bar{x}_1}{d\bar{t}} = \bar{x}_2 \qquad (50)$$

$$\frac{d\bar{x}_2}{d\bar{t}} = \bar{x}_1 \bar{x}_4^2 - \frac{1}{\bar{x}_1^2} - \frac{\bar{D}\bar{x}_2}{\bar{m}\bar{v}} + \frac{\bar{T}}{\bar{m}}\sin\alpha \qquad (51)$$

$$\frac{d\bar{x}_3}{d\bar{t}} = \bar{x}_4 \qquad (52)$$

$$\frac{d\bar{x}_4}{d\bar{t}} = -\frac{2\bar{x}_4 \bar{x}_2}{\bar{x}_1} - \frac{\bar{D}\bar{x}_4}{\bar{m}\bar{v}} + \frac{\bar{T}}{\bar{x}_1 \bar{m}}\cos\alpha \qquad (53)$$

16

$$\frac{d\bar{x}_s}{d\bar{t}} = -\bar{p}\bar{T} \qquad (54)$$

C. PROGRAM EXECUTION

Program execution begins with the input of variables from the user as well as an input file (see Appendix A). Following the definition of the initial conditions, the DRAG subroutine is called. The first call establishes the drag of the FKT benchmark. Execution then enters the main loop, where drag is called again, computing the instantaneous velocity as well as the density. With the velocity updated, the specific energy is computed and the CONTROL subroutine is called. This routine controls thruster activation and cut-off. With a thrust value thus determined, subroutine EQN updates the equations of motion. RK4 is the fourth order Runge-Kutta routine that integrates the state variables. Flight-path angle, fuel-burned totals and achieved altitudes are updated once every radian, while the routine ORBELMTS updates the classical orbital elements. The equations of motion are updated 5000 times per orbit, while all pertinent variables are sampled ten times per orbit.

D. VALIDATION

Since the program logic remains intact, the validation process is simplified. The initial baseline test consists of running the program with the spacecraft in an initially circular orbit with gravity the only external force. Radius, velocity, specific energy and angular momentum all remain constant, validating the basic equations without drag or thrust.

The next step in the validation process compares the trajectory produced by the modified version with those produced by the earlier program for a consistent set of inputs. Since an in-depth validation is done by Wilsey [Ref. 4], duplicating the results of the earlier version validates the modified program. The main difference between the two versions lay in the nondimensionalizing process, and the calculating of instantaneous spacecraft mass. To

17

achieve universality, all input variables and parameters are already nondimensionalized. Using input values which correspond to those used in the earlier study, the modified version produces equivalent results.

E. DEVELOPMENT OF "SMART" VERSION

The aim of this study is to determine values of δr and E_{th} which will maintain a specified band, therefore a version of the program that accepts input values of δr and E_{th} to simulate the trajectory is developed. This program is used as a test to validate the results obtained using the parameter mapping procedure. A listing of the program is found in Appendix C, while example input and output files are listed in Appendix D.

IV. PARAMETER MAPPING

To remove the iteration on δr and E_{th} which is required in the algorithm, a way of

determining these control parameters for a given band prior to program execution is

required. In addition, the variations in the control parameters for different spacecraft

configurations must be known.

To achieve these goals and possibly find a mathematical relationship between the

parameters, a mapping technique is used. Running the simulation for a specific spacecraft

configuration produces a set of trajectories. Multiple simulation runs for various

configurations produces a family of trajectory curves. Combining all of the trajectories into

a catalog where the achieved band is graphed against δr and E_{th} would bypass the

algorithm's iteration process; for a given spacecraft configuration and a desired orbital band,

values for δr and E_{th} could be pulled from the maps and input into the control program.

A. PARAMETER VARIATION

For this work, a spacecraft configuration is defined as a set of the three

nondimensionalized parameters previously introduced. Five values for each parameter are

combined to produce a database of 125 different configurations. The parameter values and

their dimensionalized counterparts are listed in Table 1. These values are chosen to

represent a range of actual values for thrust-to-drag ratio, ballistic coefficient and specific

impulse (I_{sp}). Increasing values of T/D represent moving up to more powerful motors.

Increases in specific impulse, the amount of thrust per unit weight of propellant, are

reflected in decreasing values of $\bar{p}$. The I_{sp} values reflect those of different propellent

19

systems, from cold gas propellants ($I_{sp} \approx 100$), to ionic propulsion systems ($I_{sp} \approx 3000$).

Increasing values for $\bar{B}$, the nondimensionalized ballistic coefficient, represent an increase in

Table 1 PARAMETER VALUES FOR MAPPING PROCEDURE

	T/D	$\bar{B}$ (B)	$\bar{p}$ (I_{sp})
1	50	8.013e3 (50)	7.902e0 (100)
2	75	1.202e4 (75)	3.161e0 (250)
3	100	2.404e4 (150)	1.581e0 (500)
4	250	4.808e4 (300)	7.902e-1 (1000)
5	500	8.013e4 (500)	2.634e-1 (3000)

spacecraft mass, decrease in surface area, or both, according to equations 35 a and b. A

representative large orbiting platform with the following characteristics

$$\text{mass} = 20,000 \text{ kg}$$
$$\text{surface area} = 60 \text{ m}^2$$
$$\text{drag coefficient} = 2.2$$

would have a ballistic coefficient of 150 kg/m².

B. PROGRAM MODIFICATION

Two modified versions of the computer simulation are used to accomplish the mapping.

One tracks the nondimensionalized orbital decay, $\delta \bar{r}$, while the other focuses on the thruster

cut-off energy, $\bar{E}_{th}$.

1. Automatic variation of ordered band

Both control parameters, $\delta \bar{r}$ and $\bar{E}_{th}$, can be defined by an "ordered" band. The

amount of orbital decay defines the lower bound, while the thruster cut-off energy defines

the upper bound. By varying this ordered band, a range of values for $\delta\bar{r}$ and $\bar{E}_{th}$ can be simulated and mapped. A program loop added outside of all subroutine calls and data output commands automated repetition of the simulation, allowing the ordered band to vary from 50 km to 0 km (which would simulate the FKT), in 2.5 km increments. For each ordered band, the program simulated 50 orbits, or approximately three days of spacecraft flight.

2. "Bubble sort" of minimum and maximum radii

The actual band of a trajectory is defined as the radial distance between the minimum and maximum radii that is achieved during the simulation. Two nondimensionalized variables, $\bar{r}_{mn}$ and $\bar{r}_{mx}$ are initially defined as equal to the initial orbit radius. As the program simulates the trajectory and the instantaneous orbit radius is computed, it is compared to the two variables. Whenever the instantaneous radius is less than the radius held in $\bar{r}_{mn}$, the variable takes on this new, lesser radius. Conversely, $\bar{r}_{mx}$ is updated to the instantaneous radius whenever the orbit goes above the current maximum. At the end of a trajectory simulation, $\bar{r}_{mn}$ and $\bar{r}_{mx}$ will hold the minimum and maximum radii achieved. The variables are reset for each trajectory, producing an actual band corresponding to each variation in $\delta\bar{r}$ and $\bar{E}_{th}$

3. Actual band vs. ordered band

The purpose of the "ordered" band is tutorial; it provides a way to visualize and vary the control parameters $\delta\bar{r}$ and $\bar{E}_{th}$. Once the simulation is run, the ordered band has no real significance. The actual radial band that is achieved for the given set of control parameters is all that is of practical interest. An orbit maintenance problem as developed here is defined by the band to be maintained, not the individual obit radii. Any specified minimum and

21

maximum orbit radii form a radial band. By looking at the achieved band rather than the minimum and maximum radii separately, the dimension of the problem is reduced.

C. MAPPING ACTUAL BAND VS. δr̄ AND Ē$_{th}$

Output from each of the parameter-mapping versions consists of the values of the respective control parameter and the corresponding actual band produced. An example plot for thruster cut-off energy is shown in Figure 4. This depiction of the trajectory is then combined with similar trajectory curves corresponding to different spacecraft configurations, producing a catalog of trajectories. With a specific spacecraft and a required band to be maintained, values of the control parameters δr̄ and Ē$_{th}$ can be pulled from the

plots and used to maintain the spacecraft's orbit, removing the need for iteration in the proposed algorithm.
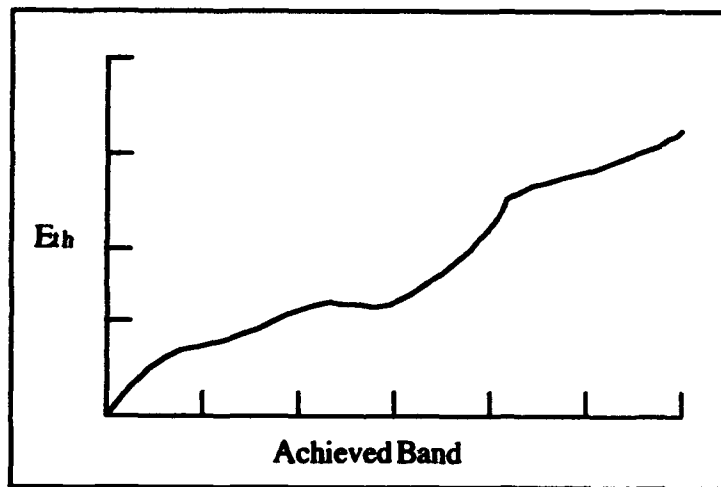
Figure 4 Example map of achieved band vs. thruster cut-off energy

22

V. ANALYSIS AND RESULTS

Analysis of the parameter maps consists of investigating the effects of spacecraft parameter variation on achieved band. While 125 different spacecraft configurations are catalogued, investigation is focused on four configurations which best exhibit the noted phenomena. The following configurations are studied:

<u>Config 533</u>	<u>Config 234</u>	<u>Config 342</u>	<u>Config 453</u>
T/D = 500	T/D = 75	T/D = 100	T/D = 250
B = 150 kg/m²	B = 150 kg/m²	B = 300 kg/m²	B = 500 kg/m²
I_{sp} = 500 sec	I_{sp} = 1000 sec	I_{sp} = 250 sec	I_{sp} = 500 sec

The prefix D- or E- on the maps indicate the source file of the data; D represents actual band plotted against orbital decay ($\delta\bar{r}$), while E represents actual band plotted against thruster cut-off energy $\left(\bar{E}_{tb}\right)$. The first digit refers to T/D ratio, the second to B, and the third to I_{sp}. On each plot, only one parameter is varied.

Accuracy of the mapping technique is also tested by using the control parameters in the "smart" version of the simulation and noting the size of the actual band achieved. All figures discussed are located in Appendix E.

A. VARIATION OF SPECIFIC IMPULSE, I_{sp}

Figures 1 through 4 show the effects of varying a spacecraft engine's specific impulse. In all cases, the effect of varying I_{sp} is extremely small. Figure 1 shows no variation between trajectories. It is also noted that the curves for actual band vs. $\delta\bar{r}$ exactly match the shape of

23

the actual band vs. $\bar{E}_{th}$. This is due to the way the control parameters are varied together, using the concept of the "ordered" band introduced in the previous chapter.

Figures 2, 3, and 4 all show families of trajectory curves corresponding to spacecraft whose configurations differ only in the value of their engine's specific impulse; thrust-to-drag ratio and ballistic coefficient remain constant within each figure. While individual trajectories differ, the general shape in each case remains the same. Also, as the actual band narrows, the trajectories become practically identical. This convergence represents identical control parameters producing equivalent bands for different spacecraft configurations.

Recalling the definition of the mass/thrust parameter $\bar{p}$ (equation 39) and Table 1 it is clear that despite large changes in specific impulse, the parameter $\bar{p}$ remains a small number that varies little. Figures 1 through 4 confirm that variations in specific impulse have little effect on the orbital band maintained using the single-burn algorithm.

B. VARIATION OF BALLISTIC COEFFICIENT

Figures 5 through 8 show the effects of varying the spacecraft's ballistic coefficient. Again, the values of thrust-to-drag ratio and (in these cases) specific impulse remain constant throughout each figure. Comparing the trajectories in any of the individual maps shows considerably more effect on actual band by variation of ballistic coefficient than was produced by varying specific impulse.

Generally, the size of the actual band for a given control parameter decreases with increasing values of the nondimensionalized ballistic coefficient. Figure 5 shows this trend with only small deviations. Figures 6 and 7 show larger variations between individual trajectories, but the shrinking of the actual band does continue. Figure 8 shows less variation, which points towards a relationship between the ballistic coefficient and the thrust-

24

to-drag ratio. Varying ballistic coefficient has less of an influence on configurations with larger values of T/D.

Recalling equations 35 and 36, increasing spacecraft mass or reducing spacecraft surface area leads to an increase in ballistic coefficient, which in turn decreases drag. As the thrusters modeled in this simulation operate at a constant thrust, those configurations with large thruster values feel little effect from the decrease in drag, while those with smaller thrusters, and thus smaller T/D ratios, more easily "sense" the decreased drag. With thrust and drag smaller, the algorithm is better able to control the actual band.

C. VARIATION OF THRUST-TO-DRAG RATIO

Figures 9 through 12 show the effects of varying the spacecraft's thrust-to-drag ratio. Each plot represents a family of spacecraft with consistent values of ballistic coefficient and specific impulse, but different T/D ratios. Comparing individual trajectory curves within a map shows that increasing thruster size generally increases the actual orbital band achieved.

As with ballistic coefficient variation, the effects of varying T/D are more profound than when changing specific impulse. Once again, the effect of large thrusters is most noticeable, as they seem to cancel out irregularities present in configurations possessing smaller thrusters. In each figure, the trajectory corresponding to that configuration with the largest thrust-to-drag ratio (T/D = 500) is a smooth curve, and in some cases almost a straight line. Larger values for T/D ratio inhibit the single-burn algorithm; for a given value of either control parameter, a larger thruster produces a larger band. Smaller thrusters, which may be thought of as being more responsive to this control scheme, produce a tighter orbital band.

D. MULTIPLE TRAJECTORIES FOR A SPECIFIED BAND

An assumption made during the formulation of the single-burn algorithm and the mapping procedure covered here deals with the relationship between the control parameters

25

and the band they produce. Given a spacecraft and a set, periodic thruster firing schedule (defined values of $\delta \bar{r}$ and $\bar{E}_{th}$), a certain radial band will be maintained. The parameter mapping technique essentially reverses this process, starting with the required radial band and looking at the required thrusting scheme.

It seems reasonable to assume that since a unique thruster firing schedule produces a specific radial band, the converse will also hold; a certain radial band will yield unique values of $\delta \bar{r}$ and $\bar{E}_{th}$. As can be seen in Figures 2 through 12, this is not the case. On each map, there is a region where a specific band can be produced by multiple values of each control variable. Such a choice between control parameter values could lead to new optimizing opportunities: which trajectory is "best"? To investigate this development, the "smart" version of the simulation is used to study different thruster firing schedules for a specific spacecraft configuration.

E. "SMART" PROGRAM VALIDATION

Figure 13 shows the two plots relating actual band to the control parameters for Configuration 234 introduced previously. For nondimensionalized radial bands between approximately .0076 and .0095 times the base orbit radius, there are three possible values for both control parameters. To validate the smart program and investigate the control parameter relationships, the following trajectories are chosen which produce nearly equal radial bands:

Trajectory	Actual band
Traj.1	0.008610134
Traj.2	0.008608818
Traj.3	0.008789484

The values of $\delta \bar{r}$ and $\bar{E}_{th}$ corresponding to each trajectory are used by the smart program to generate the specific simulation for 50 orbits.

1. Trajectory comparison

The orbit radius of each individual trajectory is shown in Figures 14 through 16. A combined plot is shown in Figure 17. While each trajectory produces a radial band of comparable width, the bands and the thruster firing patterns are quite different. Figure 14 shows Trajectory 1's decay to initial thruster firing taking just over ten orbits, followed by a long burn. After thruster cut-off the orbit's eccentricity is quite significant, as seen in the rhythmic variation in nondimensionalized radius (Rbar) as the orbit decays again to $\bar{r}_{th}$.

Figure 15 shows a similar pattern for Trajectory 2, with a smaller orbital decay and a shorter burn-time.

Figure 16 shows a much different pattern. Decay to the initial thruster firing occurs rather quickly, with the orbit proceeding directly to a highly eccentric state. The eccentricity of the orbit causes the spacecraft to hit the specified thrusting radius as well as the thruster cut-off energy more frequently. The orbit actually becomes an ellipse whose apogee and perigee are bounded by the minimum and maximum radii of the orbital band. Noting the minimum and maximum radius values for Trajectory 3 plotted in Figure 16 and the definition of eccentricity

$$ e = \frac{\bar{r}_{mx} - \bar{r}_{mn}}{\bar{r}_{mx} + \bar{r}_{mn}} \tag{55} $$

the eccentricity is found to be approximately 0.0043. Figure 18 compares the eccentricities of the three trajectories, and that of Trajectory 3 confirms the computed result, as it tends towards a steady-state value of approximately 0.0045.

27

2. Efficiency comparison

Given these differing burn patterns, which one is best? A performance index must be defined to be optimized; this study looks at maximizing fuel efficiency. Figure 19 shows the mass of fuel burned for each trajectory, as well as that for a Forced Keplerian Trajectory.

It is clear that the conclusions made by Wilsey [Ref. 4] are confirmed; none of the single-burn trajectories are more fuel-efficient than an FKT. What is of interest, however, is that the average slope of the fuel-burned curve appears independent of thruster burn pattern. Regardless of the frequency and length of thruster firing, all three single-burn algorithm produce the same average fuel burn rate.

3. Variation Of Orbital Simulation Length

In comparing these trajectories, it is helpful to look at different orbital parameters, including spacecraft specific energy. The nondimensionalized specific energy is defined as

$$\bar{\varepsilon} = \frac{\bar{v}^2}{2} - \frac{1}{\bar{r}} \qquad (56)$$

and is shown for each orbit in Figure 20. The near vertical increases in specific energy correspond to thruster firings; the greater the rise in energy, the longer the burn. Trajectory 3 quickly reaches a state where the specific energy is tightly controlled by a high-frequency, short-burn schedule. With only two burns showing for the other trajectories, however, sound conclusions cannot be drawn; more data is required. An additional series of simulations is run for a period of 100 orbits, with orbit radius, specific energy, and fuel mass burned shown in Figures 21 through 24, respectively.

a. *Transition to a Tight Energy State*

From Figure 21, it is seen that Trajectory 2 undergoes a significant change around its 65th orbit; the radial band maintained expands significantly. Comparing the three trajectories in Figure 22, it is seen that Trajectory 2 transitions to a tightly governed energy state very similar to that reached earlier by Trajectory 3 (although the energy level of Trajectory 2 is higher). This transition appears due to the eccentricity of the orbit increasing to a point where the orbit grazes the prescribed band; the perigee and the apogee of the orbit are consistently in contact with the bounds defined by the control parameters, as shown in Figure 23. Despite the change in the thrusting pattern and the increase in radial band size, Figure 24 shows that the slope of the fuel-burned curve remains consistent, above that of the FKT.

VI. CONCLUSIONS AND RECOMMENDATIONS

The purpose of this thesis was to create a catalog of control parameter maps for various spacecraft configurations, using a proposed single-burn trajectory algorithm for low-earth orbit maintenance. Such maps are used to remove the iteration required in the algorithm (Appendix A), assuring maintenance of the desired band and removing the need for human intervention in the control process. Additionally, study of the relationships between control and spacecraft configuration parameters led to new insights into the orbit maintenance problem. Finally, comparison of all single-burn trajectories to the Forced Keplerian Trajectory (FKT) benchmark for optimization of fuel-efficiency could not corroborate the optimal control theory finding that the FKT is not the optimal trajectory.

The FORTRAN simulation developed by Pauls [Ref. 3] and refined by Wilsey [Ref. 4] was further modified by nondimensionalizing the entire simulation, then developing two versions to accomplish the parameter mapping. A "smart" version was also developed which would accept as input the control parameters mapped out in the thesis, thus testing the validity of the plots.

Three nondimensionalized spacecraft configuration parameters related to thrust-to-drag ratio, ballistic coefficient, and specific impulse were defined and varied through a range practical values. Their individual effects upon the spacecraft's trajectory were studied. Variations in specific impulse produced little change in the trajectories. Variations in ballistic coefficient and thrust-to-drag ratio produced more pronounced changes between trajectories, with a coupling noted between the two. While increasing the value of the ballistic coefficient generally decreased the size of the maintained band, the influence of the ballistic coefficient was significantly reduced for high thrust values. High values of T/D

30

produced larger radial bands, and also seemed to cancel out any orbital irregularities present in spacecraft with smaller, less powerful thrusters.

An interesting discovery was that a specific radial band could be produced by different combinations of control parameters; the relationship between an orbital band and a thruster firing schedule was not one-to-one. This allowed for further optimization studies, as a certain single-burn scheme might actually be superior to an FKT.

While the FKT was shown to be consistently better than all single-burn trajectories in this study, the differences in thruster firing patterns proved intriguing. Different trajectories producing comparable radial bands had drastically different thruster firing times and frequencies. High orbit eccentricity, where the orbit's perigee and apogee were bounded by the radial band , sent the trajectory into a periodic, high-frequency, low burn-time thrusting scheme, where specific energy varied little. Fuel-burn curves for each single-burn trajectory maintained a consistent slope, even after the orbit transitioned to this tightly governed specific energy state.

This thesis opens the door for further study as well, since some questions were unanswered, and new questions have arisen. A comparison of the single-burn algorithm to a dual-burn algorithm such as EITAG [Ref. 2] is warranted. While not superior to an FKT, a single-burn orbit maintenance algorithm may still be better than the dual-burn solution. Additionally, what effects do other orbital parameters such as flight-path angle and spacecraft velocity have upon the trajectory? Is the transition to the tight energy state globally valid? And on a grander scale, what is the optimal orbit maintenance strategy? What form of bang-bang control will minimize fuel burned and provide the most efficient means of maintaining a continued presence on orbit? With man's continued presence in space seemingly contingent upon maximizing performance and efficiency while minimizing cost, such study is certainly warranted.

31

APPENDIX B

Nondimensionalization Table

Quantity (=)	Parameter (*)	Factor
radius : r	RBAR	r_b
mass : m	MBAR	m_b
time : t	TBAR	t_b
velocity : v	VBAR	r_b / t_b
energy : E	EBAR	μ / r_b
thrust : T	THBAR	$m_b r_b / t_b^2$
density : ρ	RHOBAR	ρ_b
drag : D	DBAR	$m_b r_b / t_b^2$
ballistic coeff : B	BBAR	$\rho_b r_b$
mass flow : MDOT	MDOTBAR	m_b / t_b
atm scale ht : β	BETABAR	$1 / r_b$
angular momentum : h	HBAR	r_b^2 / t_b
semi-major axis : a	ABAR	r_b
thrust/drag parameter : T_d	TDBAR	TBAR / D0BAR

APPENDIX C

A. PROGRAM LISTING

```
        PROGRAM ORBMAINT
C       ORBMAINT is a self-contained, nondimensionalized orbit maintenance program
C    that will control the orbit of one body orbiting another. The program consists of a main
C    routine controlling input, output, and subroutine calls, and five subroutines which
C    compute atmospheric drag, the equations of motion, the standard orbital elements, and
C    the number and duration of thruster firings. A 4th order Runge-Kutta integrator is used
C    to solve the equations of motion. The program also performs comparative calculations
C    for a Forced Keplerin Trajectory (FKT)
C
C       VARIABLE DEFINITIONS
C          ARRAYS:
C             XBAR(1)              nondimensionalized orbit radius
C             XBAR(2)              nondimensionalized orbital radial velocity
C             XBAR(3)              theta
C             XBAR(4)              nondimensionalized orbital angular velocity
C             XBAR(5)              nondimensionalized spacecraft mass
C             XBDOT(1)             derivative of XBAR(1)
C             XBDOT(2)             derivative of XBAR(2)
C             XBDOT(3)             derivative of XBAR(3)
C             XBDOT(4)             derivative of XBAR(4)
C             XBDOT(5)             derivative of XBAR(5)
C          FILE INPUT:
C             R0BAR                initial nondimensionalized orbit radius
C             M0BAR                initial nondimensionalized spacecradft mas
C             FORBIT               number of orbits to simulate
C             STEP                 time increment step size
C             PRNT                 print interval step size
C             DETABAR              atmospheric scale height
C             TDBAR                nondimensionalized thrust-to-drag ratio
C             BBAR                 nondimensionalized ballistic coefficient
C             PBAR                 nondimensionalized mass/thrust parameter
C          USER INPUT:
C             ALPHA
C              ALPHAR              thrust angle
C             DLTRBR               nondimensionalized orbital decay: R0BAR-RTHBR
C             ETHBR                nondimensionalized spacecraft energy
C          COUNTERS:
C             TBAR                 current time (initial value = 0)
C             INDEX                (initial value = 0)
C             KOUNT                (initial value = 0)
```

```
C          INITIAL AND BOUNDARY CONDITIONS:
.C              DOBAR                    initial nondimensionalized atmospheric drag
C              EOBAR                    initial nondimensionalized spacecraft energy
C              VOBAR                    initial nondimensionalizedspacecraft velocity
C              RMNBR                    nondimensionalized minimum orbit radius
C              RMXBR                    nondimensionalized maximum orbit radius
C          PROGRAM VARIABLES:
C              ABAR                     nondimensionalized semi-major axis
C              APOGEE                   nondimensionalized orbit apogee
C              DBAR                     nondimensionalized atmospheric drag force
C              EBAR                     nondimensionalized spacecraft energy
C              ECC                      orbital eccentricity
C              GAMMAD
C              GAMMAR                   flight path angle
C              HBAR                     nondimensionalized angular momentum
C              FUELKEP                  keplerian fuel burned per program iteration
C              TOTKEP                   total keplerian fuel burned
C              MBRFUEL                  nondimensionalized mass of fuel burned
C              PERIGEE                  nondimensionalized orbit perigee
C              PRDBAR                   nondimensionalized orbit period
C              RHOBAR                   nondimensionalized atmospheric density
C              RTHBR                    nondimensionalized radius of thruster firing
C              TBARF                    simulation stop time
C              THBAR                    nondimensionalized spacecraft thrust
C              THBRCAP                  nondimensionalized spacecraft thrust capability
C              THBRKEP                  nondimensionalized keplerian thrust
C              THGMA                    flight path angle at thruster initiation
C              VBAR                     nondimensionalized spacecraft velocity
C          CONSTANTS:
C              PI                       pi
C              J                        state variable index
C
C     variable declarations:
          IMPLICIT REAL*8(A-H,M-Z)
          DIMENSION XBAR(5),XBDOT(5)
C
C     constant definitions:
          PI=DATAN(1.0D+00)*4.0D+00
          J=5
C
C     initialize keplerian fuel totals
          FUELKEP=0.0D+00
          TOTKEP=0.0D+00
CCCCCCCCCCCCCCCCCCCCCCCCC
C
          OPEN(10, FILE='input', STATUS='OLD')
          OPEN(20, FILE='orbpar', STATUS='NEW')
          OPEN(30, FILE='orbel', STATUS='NEW')
          OPEN(40, FILE='orbetc', STATUS='NEW')
C
```

35

```
C      read input file
       READ(10,1) R0BAR,M0BAR,FORBIT,STEP,PRNT,BETABAR,
      *TDBAR,BBAR,PBAR
1      FORMAT(10(/,21X,D15.9))
C
C      convert time and intervals to radians
       TBARF=2.0*PI*FORBIT
       STEP=2.0*PI*STEP
       PRNT=2.0*PI*PRNT
C
C      read user inputs of thrust angle and control parameters
       PRINT*, 'ENTER ALPHA'
       READ*, ALPHA
       ALPHAR=ALPHA*PI/180.0D+0
C
       PRINT*, 'ENTER DLTRBR'
       READ*, DLTRBR
C
       PRINT*, 'ENTER ETHBR'
       READ*, ETHBR
C
       initialize counters
       TBAR=0.0D+00
       INDEX=0
       KOUNT=1
C
C      initialize state variables
       XBAR(1)=R0BAR
       XBAR(2)=0D+0
       XBAR(3)=0D+0
       XBAR(4)=(1/R0BAR)**1.5
       XBAR(5)=M0BAR
C
C      initially, set achieved orbit radii to center of orbital band
       RMNBR=R0BAR
       RMXBR=R0BAR
C
C      set radius for thruster initiation
       RTHBR=R0BAR-DLTRBR
C
C      CALCULATIONS
C
C      call DRAG to determine initial and keplerian atmospheric drag
       CALL DRAG(BBAR,XBAR,BETABAR,VBAR,DBAR)
       D0BAR=DBAR
C      commence calculation loop. call DRAG to determine s/c velocity and atm drag
100    CALL DRAG(BBAR,XBAR,BETABAR,VBAR,DBAR)
C      determine s/c energy
       EBAR=(VBAR*VBAR)/2.0-(1/XBAR(1))
C      determine spacecraft thrust capability
       THBRCAP=TDBAR*D0BAR
```

```
C     determine keplerian thrust (=atmospheric drag)
      THBRKEP=D0BAR
C     call CONTROL to fire or shutdown thrusters
      CALL CONTROL(ETHBR,XBAR,THBAR,RTHBR,EBAR,THBRCAP)
C     call EQN to update the orbital equations of motion
      CALL EQN(DBAR,XBAR,XBDOT,VBAR,THBAR,ALPHAR,PBAR)
C     call RK4 to do the runge-kutta integration over time
      CALL RK4(TBAR,XBAR,XBDOT,J,STEP,INDEX)
C
C     check for completion of runge-kutta integrator. if not done, loop back to 100
      IF (INDEX .NE. 0) GO TO 100
C     runge-kutta complete: update variables for computation of orbital elements
C     and output
      GAMMAR=ATAN(XBAR(2)/(XBAR(1)*XBAR(4)))
      GAMMAD=GAMMAR*180.0D+0/PI
C     compute flight path angle during thrusting, THGMA
      IF (THBAR .GT. 0.0D+00) THEN
              THGMA =GAMMAD
      ELSE
              THGMA=0.0D+00
      ENDIF
C
      RBAR=XBAR(1)
      MBAR=XBAR(5)
      MBRFUEL=M0BAR-MBAR
      FUELKEP=THBRKEP*PBAR*STEP
      TOTKEP=TOTKEP+FUELKEP
      IF (RBAR .LE. RMNBR) RMNBR=RBAR
      IF (RBAR .GE. RMXBR) RMXBR=RBAR
      ACTBAND=RMXBR-RMNBR
C
C     call ORBELMTS to determine the classical orbital elements
      CALL ORBELMTS(EBAR,RBAR,VBAR,GAMMAR,ECC,ABAR,APOGEE,
     *PERIGEE,PRDBAR)
C
C     check if print interval acheived. if not, skip ouput section
      IF (KOUNT .LT. DNINT(PRNT/STEP)) GO TO 200
C
C     OUTPUT
C
      WRITE(20,2)TBAR/(2.0*PI),RBAR,VBAR,MBRFUEL,EBAR
2     FORMAT(2X,F6.2,2X,F11.9,2X,F11.9,2X,F11.9,2X,F11.9)
C
      WRITE(30,3)TBAR/(2.0*PI),ABAR,ECC,APOGEE,PERIGEE,PRDBAR
3     FORMAT(2X,F6.2,1X,F11.9,3X,F8.6,3X,F11.9,1X,F11.9,2X,F8.4)
C
      WRITE(40,4)TBAR/(2.0*PI),DBAR,GAMMAD,THBAR,TOTKEP
4     FORMAT(1X,F6.2,2X,F12.9,1X,F10.4,1X,F11.9,1X,15.12)
C
C     once printing completed, reset counter
      KOUNT=0
```

```
C     update counter
200      KOUNT=KOUNT+1
C
C     check if simulation complete. if not loop back to 100
         IF (TBAR .LT. TBARF) GO TO 100
C
         PRINT*, 'Actual band achieved:  '
         PRINT*, ACTBAND
C
         END
CCCCCCCCCCCCCCCCCCCCCCC
C     DRAG calculates the spacecraft velocity and the atmospheric drag acting on the
C     spacecraft, using a local exponential atmospheric density model
C
         SUBROUTINE DRAG(BBAR,XBAR,BETABAR,VBAR,DBAR)
         IMPLICIT REAL*8(A-H,M-Z)
         DIMENSION XBAR(5)
C
C     calculate spacecraft velocity
         VBAR=((XBAR(2)*XBAR(2))+(XBAR(1)*XBAR(4))**2)**0.5
C     calculate nondimensionalized atmospheric density
         RHOBAR=EXP(-BETABAR*(XBAR(1)-1))
C     calculate nondimensionalized atmospheric drag
         DBAR=RHOBAR*VBAR*VBAR/(2.0*BBAR)
C
         RETURN
         END
CCCCCCCCCCCCCCCCCCCCCCCCC
C     EQN updates the spacecraft equations of motion
C
         SUBROUTINE EQN(DBAR,XBAR,XBDOT,VBAR,THBAR,ALPHAR,PBAR)
         IMPLICIT REAL*8(A-H,M-Z)
         DIMENSION XBAR(5) ,XBDOT(5)
C
         PI=DATAN(1.0D+00)*4.0D+00
C
         A=XBAR(1)*XBAR(4)*XBAR(4)
         B=1/(XBAR(1)*XBAR(1))
         C=DBAR*XBAR(2)/(XBAR(5)*VBAR)
         E=THBAR*SIN(ALPHAR)/XBAR(5)
C
         F=2.0*XBAR(4)*XBAR(2)/XBAR(1)
         G=DBAR*XBAR(4)/(XBAR(5)*VBAR)
         H=THBAR*COS(ALPHAR)/(XBAR(5)*XBAR(1))
C
         XBDOT(1)=XBAR(2)
         XBDOT(2)=A-B-C+E
         XBDOT(3)=XBAR(4)
         XBDOT(4)=-F-G+H
         XBDOT(5)=-PBAR*THBAR
C
```

38

```fortran
      RETURN
      END
CCCCCCCCCCCCCCCCCCCCCCCC
C     ORBELMTS calculates the nondimensionalized orbital elements
C
      SUBROUTINE ORBELMTS(EBAR,RBAR,VBAR,GAMMAR,ECC,ABAR,
     *APOGEE,PERIGEE,PRDBAR)
      IMPLICIT REAL*8(A-H,M-Z)
C
      PI=DATAN(1.0D+00)*4.0D+00
C
C     calculate angular momentum
      HBAR=RBAR*VBAR*COS(GAMMAR)
C     calculate eccentricity
      PROB=(1.0+2.0*EBAR*HBAR*HBAR)
      IF (DABS(PROB) .LT. 1.0D-12) THEN
            ECC=0.0D+00
      ELSE
            ECC=PROB**0.5
      ENDIF
C     calculate semi-major axis
      ABAR=-1.0/(2.0*EBAR)
C     calculate apogee
      APOGEE=ABAR*(1.0+ECC)
C     calculate perigee
      PERIGEE=ABAR*(1.0-ECC)
C     calculate period
      PRDBAR=2.0*PI*(ABAR**1.5)
C
      RETURN
      END
CCCCCCCCCCCCCCCCCCCCCCCC
C     RK4 does the fourth order runge-kutta integration
C
      SUBROUTINE RK4(TBAR,XBAR,XBDOT,J,STEP,INDEX)
      IMPLICIT REAL*8(A-H,M-Z)
      INTEGER INDEX,I
      DIMENSION XBAR(5),XBDOT(5),SAVED(5),SAVEX(5)
C
      INDEX=INDEX+1
      GO TO (1,2,3,4),INDEX
C
1     DO 10 I=1,J
      SAVEX(I)=XBAR(I)
      SAVED(I)=XBDOT(I)
10    XBAR(I)=SAVEX(I)+0.5D+0*STEP*XBDOT(I)
      TBAR=TBAR+0.5D+0*STEP
      RETURN
C
2     DO 20 I=1,J
      SAVED(I)=SAVED(I)+2.0D+0*XBDOT(I)
```

```fortran
20        XBAR(I)=SAVEX(I)+0.5D+0*STEP*XBDOT(I)
          RETURN
C
3         DO 30 I=1,J
          SAVED(I)=SAVED(I)+2.0D+0*XBDOT(I)
30        XBAR(I)=SAVEX(I)+STEP*XBDOT(I)
          TBAR=TBAR+0.5D+00*STEP
          RETURN
C
4         DO 40 I=1,J
40        XBAR(I)=SAVEX(I)+STEP/6.0D+0*(SAVED(I)+XBDOT(I))
          INDEX=0
          RETURN
C
          END
CCCCCCCCCCCCCCCCCCCCCCCCC
C    CONTROL determines if the spacecraft is within radial and energy limits prescribed
C    by the desired radial band and controls firing of the thrusters accordingly
C
          SUBROUTINE CONTROL(ETHBR,XBAR,THBAR,RTHBR,EBAR,
         *THBRCAP)
          IMPLICIT REAL*8(A-H,M-Z)
          DIMENSION XBAR(5),XBDOT(5)
C
C    check if thrusters already on
          IF (THBAR .EQ. THBRCAP) GO TO 100
C    check if orbit radius is less than or equal to thrusting radius
              IF (XBAR(1) .LE. RTHBR) THEN
C    check if s/c energy is less than or equal to thrusting energy
                  IF (EBAR .LE. ETHBR) THEN
C    if both are true, then fire thrusters
                      THBAR=THBRCAP
                  ELSE
C    if not, do not fire thrusters
                      THBAR=0D+0
                  ENDIF
              ELSE
                  THBAR=0D+0
              ENDIF
C
C    check if s/c energy is greater than thrusting energy. if so, turn off thrusters
100       IF (EBAR .GE. ETHBR) THBAR=0D+0
C
          RETURN
          END
C
CCCCCCCCCCCCCCCCCCCCCCCCCCCCCCCCCCCCCCCCCCCCCCCCCCCCCCCC
```

APPENDIX D

A. SAMPLE INPUT FILE

1.000000000D+00	R0BAR
1.000000000D+00	M0BAR
1.000000000D+02	FORBIT
2.000000000D-04	STEP
1.000000000D-01	PRNT
1.407286740D+02	BETABAR
7.500000000D+01	TDBAR
2.403901513D+04	BBAR
7.902309754D-01	PBAR

B. SAMPLE OUTPUT FILES (through 20 orbits)

SPACECRAFT CONFIGURATION: 234
    T/D:75   B:150   Isp:1000

REQUIRED BAND:	0.006035
DLTRBR:	0.001035681
ETHBR:	-0.499482695
ACHIEVED BAND:	0.0059946

FILE: ORBPAR

ORBIT	RADIUS	VELOCITY	FUEL BURNED	ENERGY
1.00	0.999733807	1.000133083	0.000000000	-.500133172
2.00	0.999457389	1.000271285	0.000000000	-.500271584
3.00	0.999169910	1.000415031	0.000000000	-.500415663
4.00	1.003238879	0.997268162	0.002423820	-.499499684
5.00	1.003357471	0.997127460	0.002644308	-.499522178
6.00	1.003534507	0.996949890	0.002913851	-.499523400
7.00	1.003680096	0.996803384	0.003182619	-.499524904
8.00	1.003794299	0.996688313	0.003451645	-.499526248
9.00	1.003874691	0.996606844	0.003720414	-.499527664
10.00	1.003919779	0.996560448	0.003988924	-.499529162
11.00	1.003930433	0.996548591	0.004257950	-.499530408
12.00	1.003904591	0.996572859	0.004526460	-.499531863
13.00	1.003843996	0.996631972	0.004795487	-.499533080
14.00	1.003747894	0.996726219	0.005063997	-.499534523
15.00	1.003617000	0.996855001	0.005332249	-.499536089
16.00	1.003452807	0.997016952	0.005600501	-.499537673
17.00	1.003257664	0.997209856	0.005869011	-.499539165
18.00	1.003034742	0.997430684	0.006138037	-.499540455
19.00	1.002785952	0.997677081	0.006406547	-.499543844
20.00	1.002513219	0.997947130	0.006674541	-.499543844

41

FILE: ORBEL

ORBIT	SEM-MAJ AX	ECCTCTY	APOGEE	PERIGEE	PERIOD
1.00	0.999733728	0.000002	0.999736079	0.999731376	6.2807
2.00	0.999457127	0.000005	0.999461975	0.999452278	6.2781
3.00	0.999169364	0.000008	0.999176871	0.999161858	6.2754
4.00	1.000956558	0.003012	1.004017094	0.997986175	6.2926
5.00	1.000956558	0.003013	1.003972874	0.997940243	6.2922
6.00	1.000954109	0.003008	1.003965144	0.997943075	6.2922
7.00	1.000951095	0.003003	1.003957068	0.997945122	6.2922
8.00	1.000948404	0.002999	1.003950002	0.997946805	6.2921
9.00	1.000945566	0.002995	1.003943187	0.997947945	6.2921
10.00	1.000942563	0.002991	1.003936143	0.997948982	6.2921
11.00	1.000940067	0.002988	1.003930476	0.997949658	6.2920
12.00	1.000937151	0.002985	1.003924458	0.997949844	6.2920
13.00	1.000934713	0.002982	1.003919724	0.997949702	6.2920
14.00	1.000931822	0.002980	1.003914742	0.997948902	6.2920
15.00	1.000928684	0.002978	1.003909285	0.997948082	6.2919
16.00	1.000925510	0.002975	1.003903572	0.997947449	6.2919
17.00	1.000922520	0.002973	1.003898246	0.997946794	6.2919
18.00	1.000919936	0.002972	1.003894303	0.997945570	6.2919
19.00	1.000916822	0.002971	1.003890236	0.997943408	6.2918
20.00	1.000913145	0.002969	1.003884904	0.997941385	6.2918

FILE: ORBETC

ORBIT	DRAG	GAMMA	THRUST	FKT FUEL
1.00	0.000021599	-0.0001	0.000000000	0.000103273109
2.00	0.000022462	-0.0003	0.000000000	0.000206546218
3.00	0.000023396	-0.0004	0.000000000	0.000309819327
4.00	0.000013114	0.1157	0.000000000	0.000413092436
5.00	0.000012893	0.1045	0.000000000	0.000516365544
6.00	0.000012571	0.0888	0.000000000	0.000619638653
7.00	0.000012313	0.0721	0.000000000	0.0007722911762
8.00	0.000012114	0.0546	0.000000000	0.000826184871
9.00	0.000011975	0.0365	0.000000000	0.0009929457980
10.00	0.000011899	0.0179	0.000000000	0.001032731089
11.00	0.000011880	-0.0009	0.000000000	0.001136004198
12.00	0.000011924	-0.0197	0.000000000	0.001239277307
13.00	0.000012028	-0.0382	0.000000000	0.001342550415
14.00	0.000012194	-0.0563	0.000000000	0.001445823524
15.00	0.000012424	-0.0737	0.000000000	0.001549096633
16.00	0.000012718	-0.0902	0.000000000	0.001652369742
17.00	0.000013078	-0.1056	0.000000000	0.001755642851
18.00	0.000013500	-0.1197	0.000000000	0.001858915960
19.00	0.000013988	-0.1324	0.000000000	0.001962189069
20.00	0.000014543	-0.1434	0.000000000	0.002065462178

APPENDIX E

Trajectory Maps
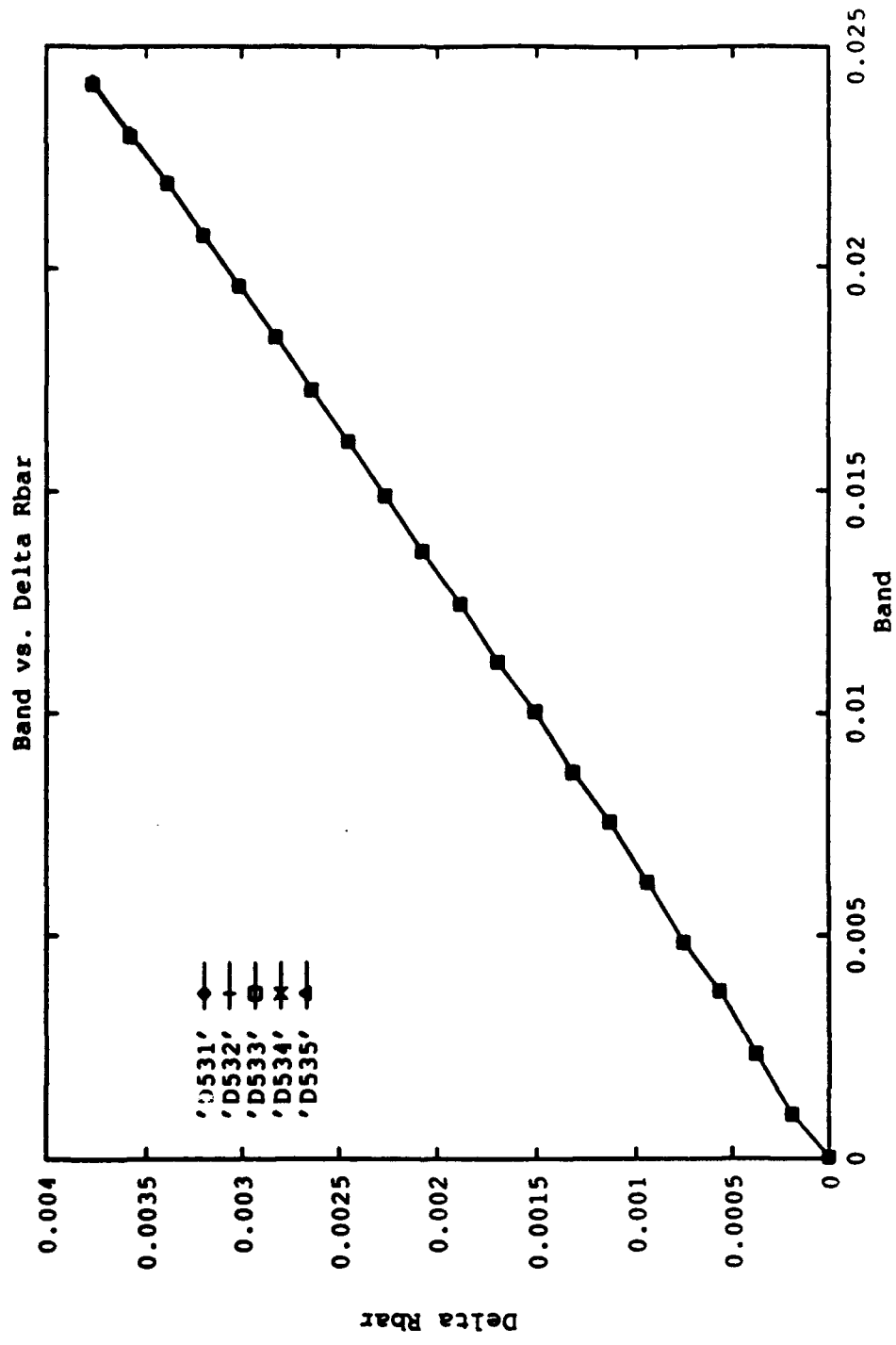
Figure 1a
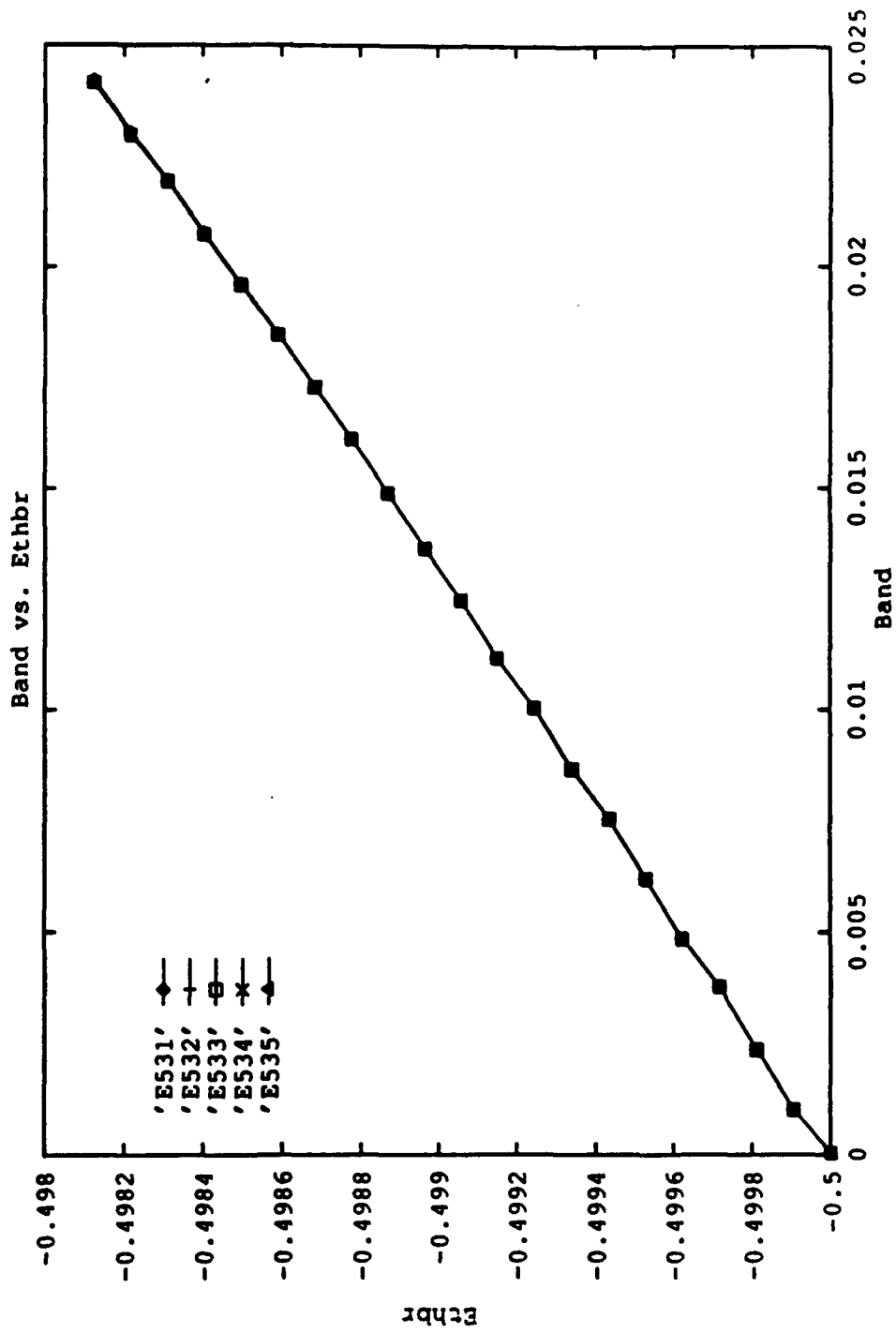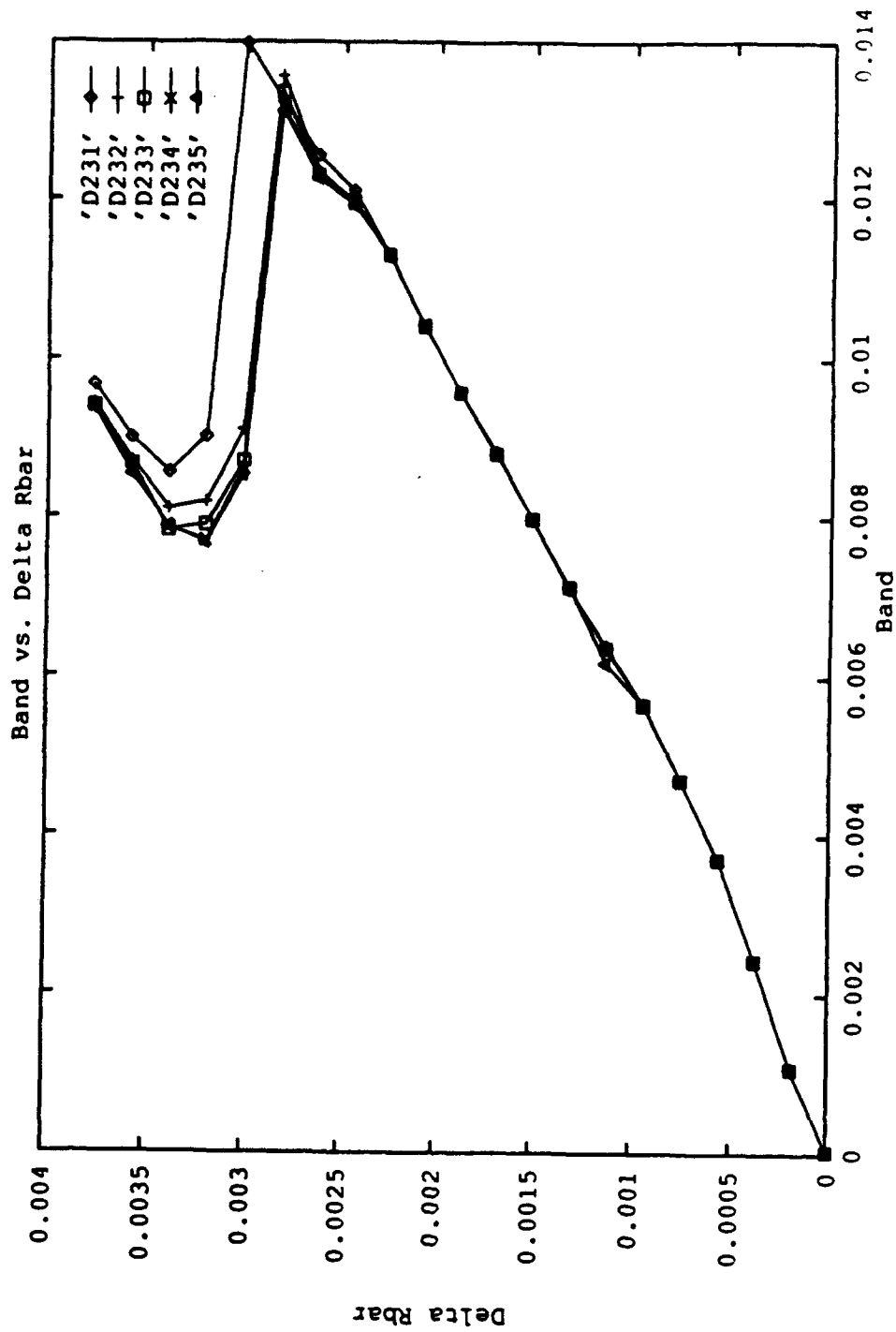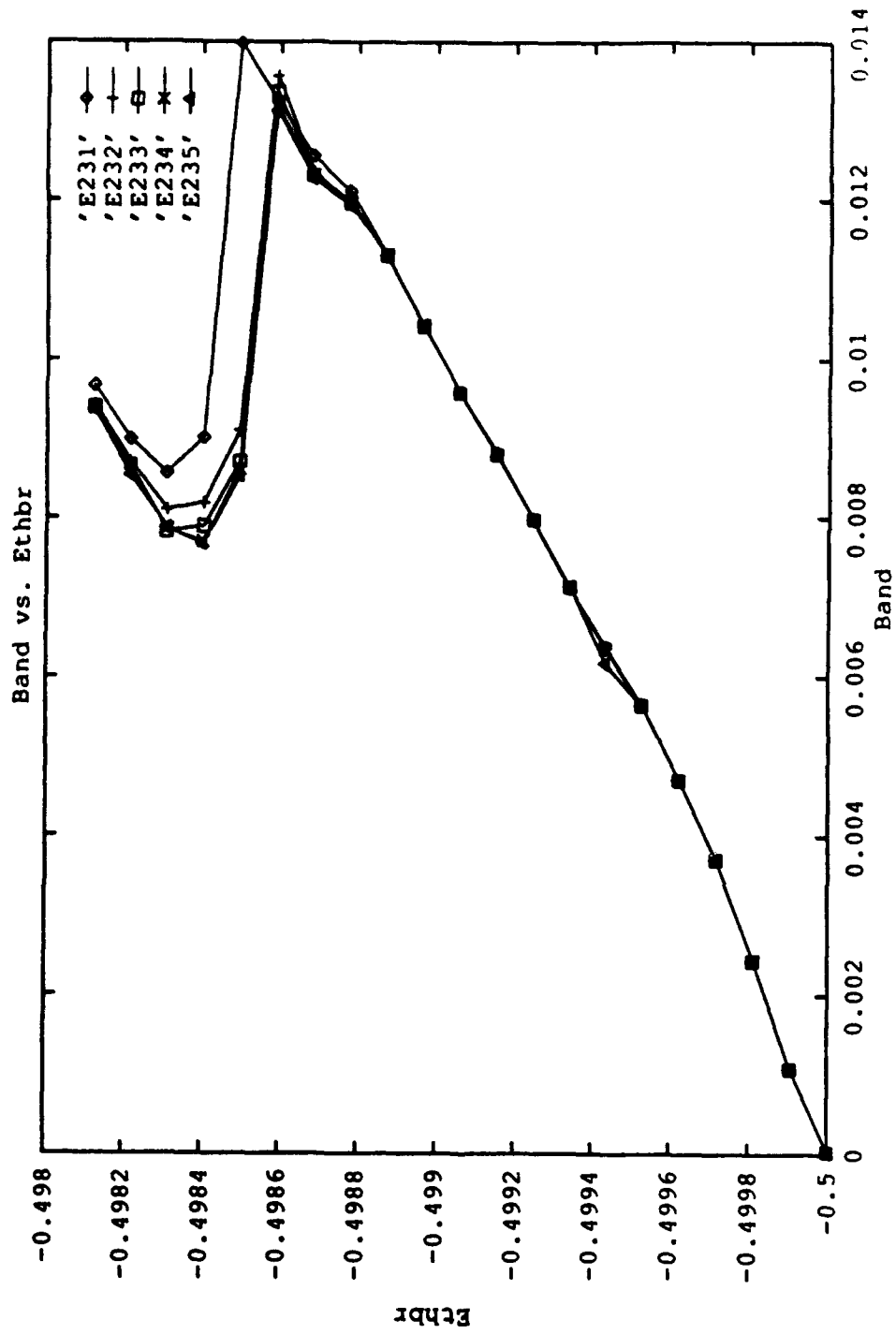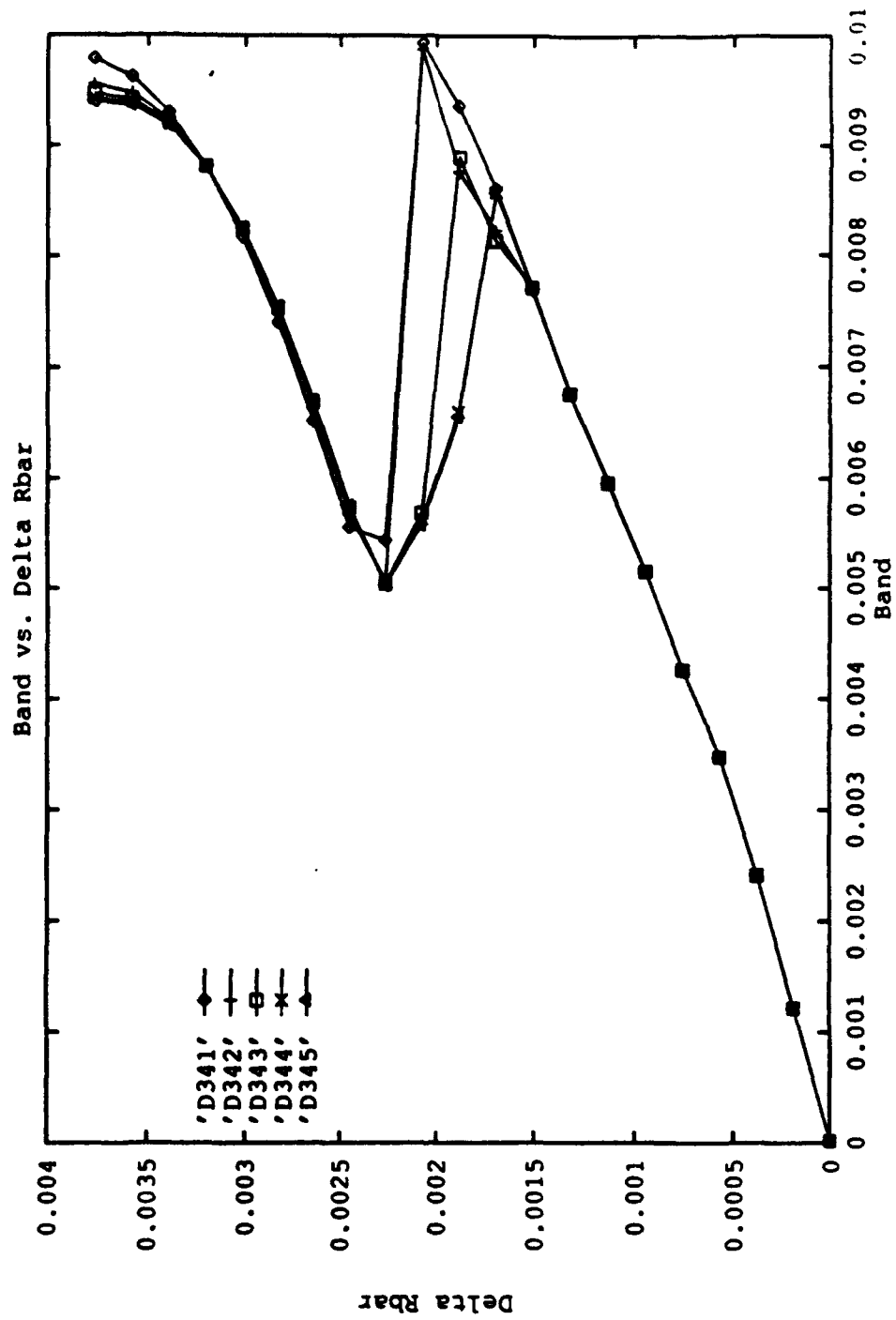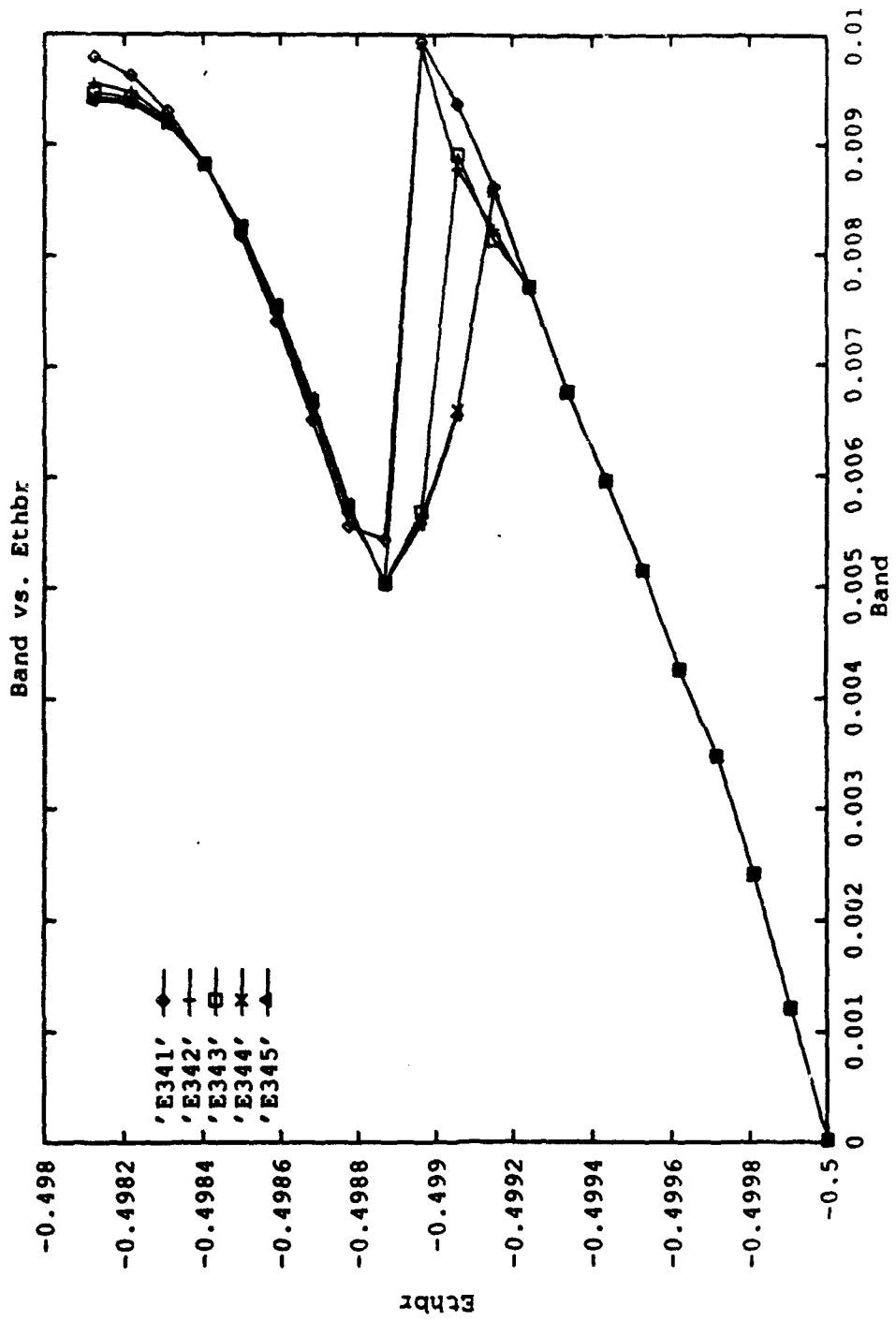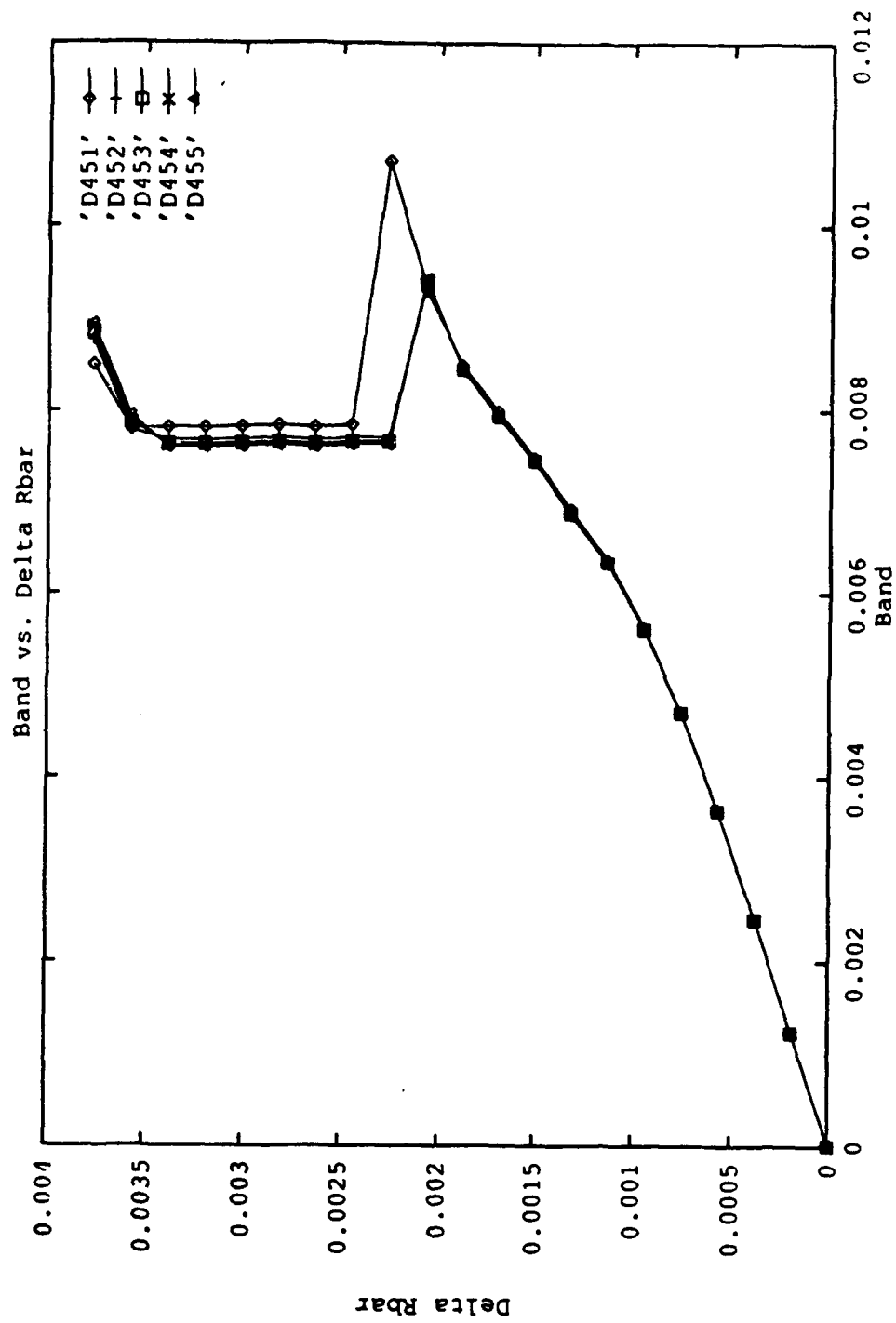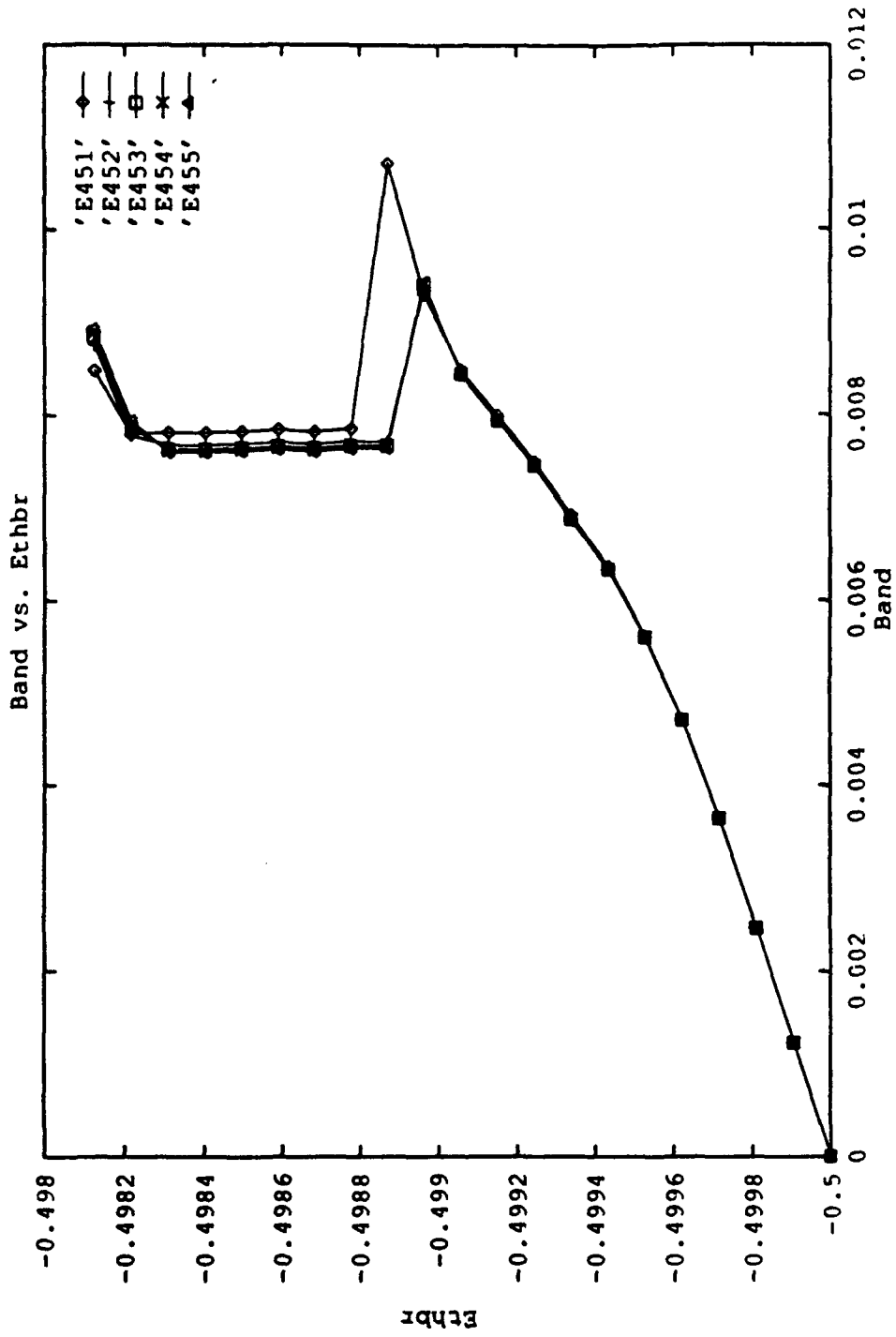
44

Figure 1b

45

Figure 2a

46

Figure 2b

47

Figure 3a

48

Figure 3b

49

Figure 4a

Figure 4b
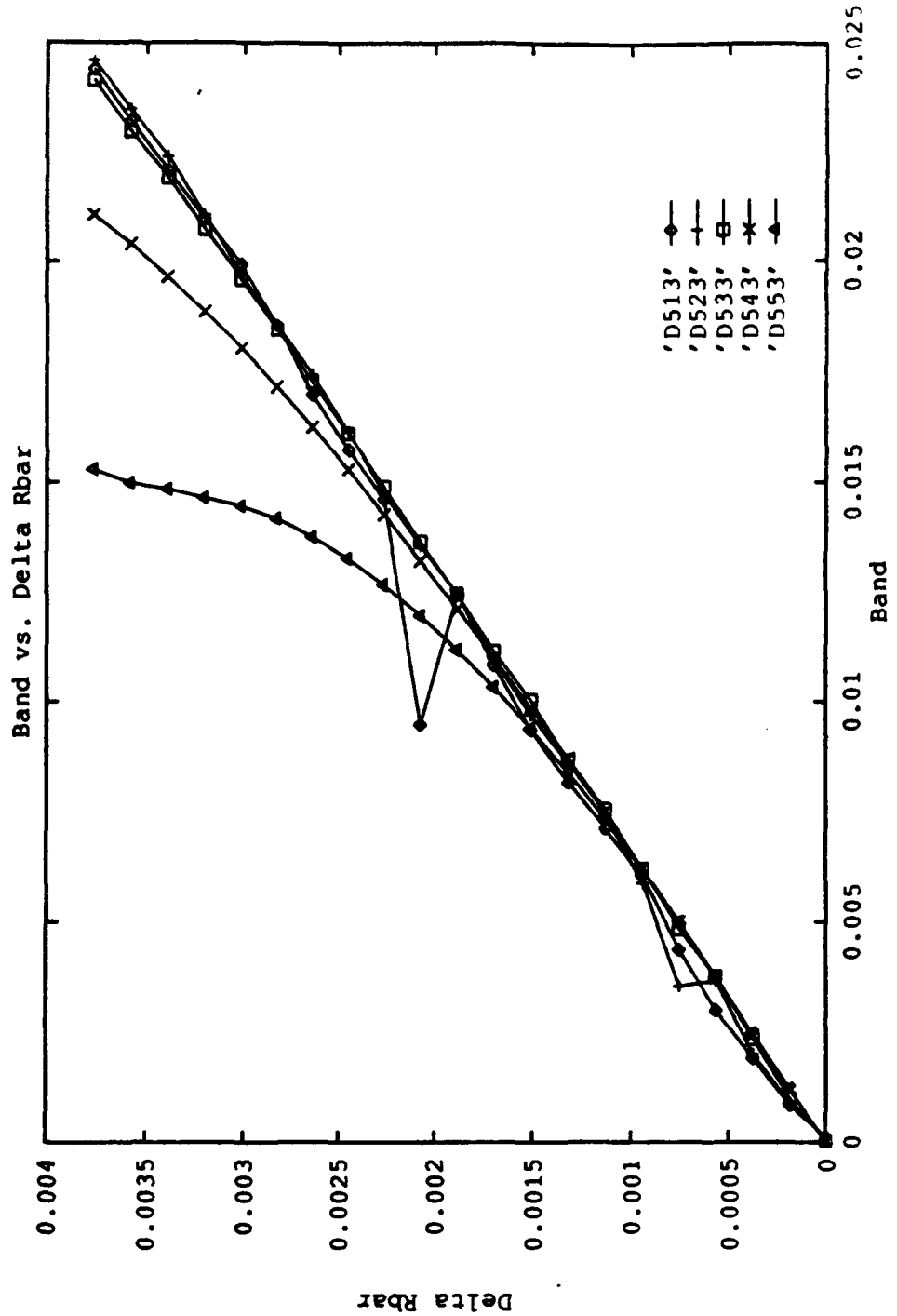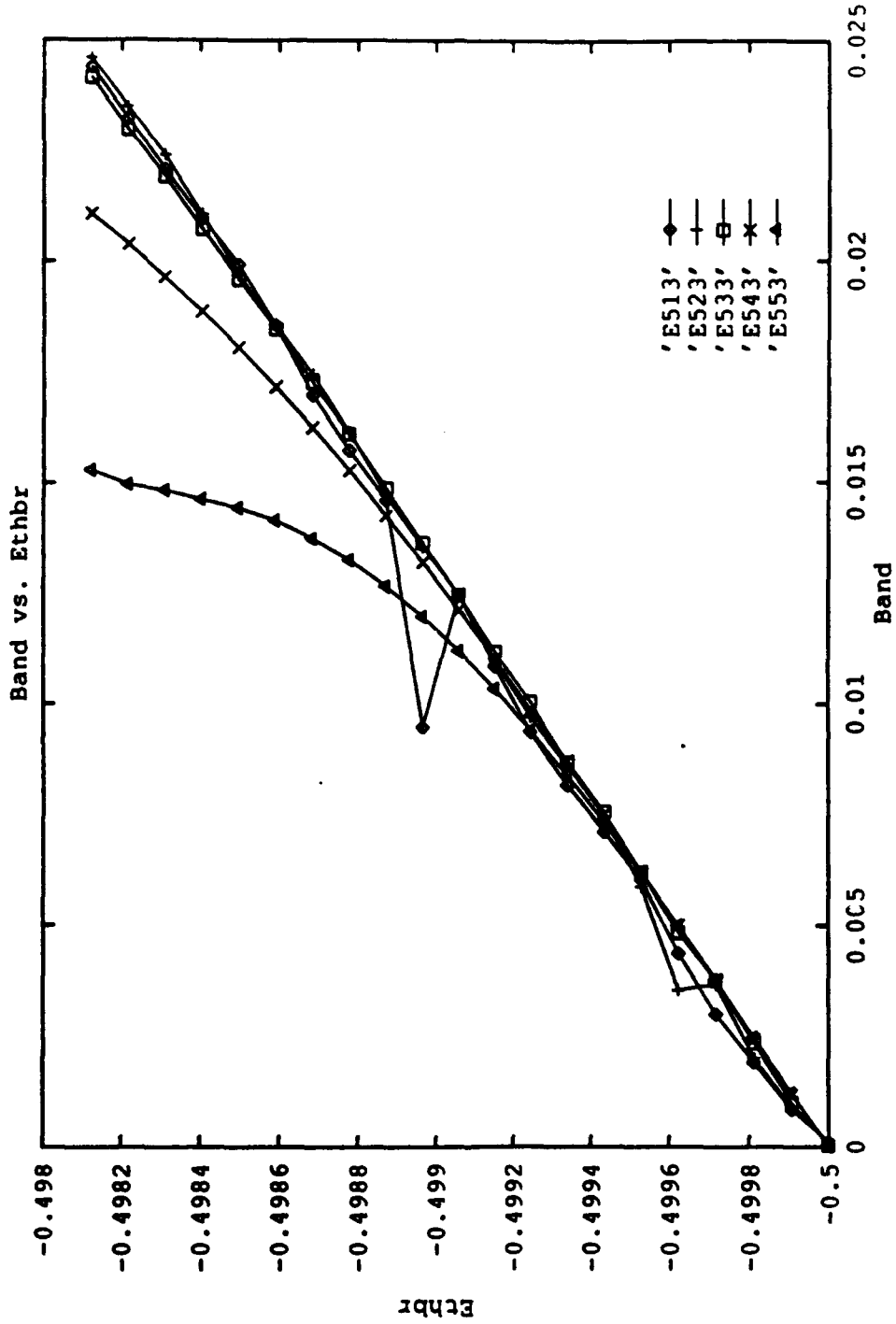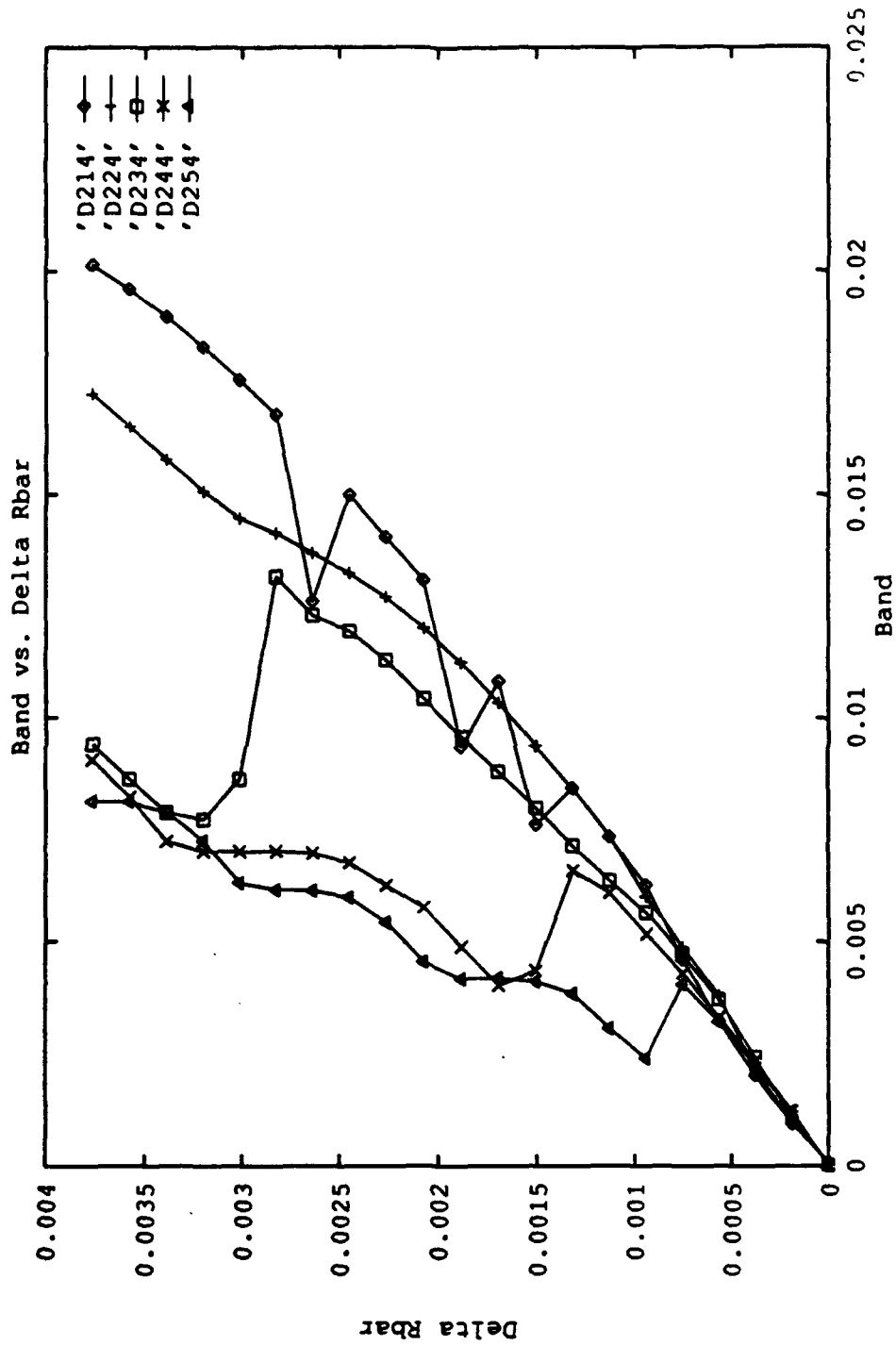
51

Figure 5a

52

Figure 5b

53

Band vs. Delta Rbar

Figure 6a

54

Figure 6b

55

Figure 7a

56

Figure 7b

Band vs. Delta Rbar

Figure 8a

Figure 8b

59

Figure 9a

60

Figure 9b

Figure 10a

62

Figure 10b

63

Band vs. Delta Rbar

'D142'
'D242'
'D342'
'D442'
'D542'

Figure 11a

64

Figure 11b

65
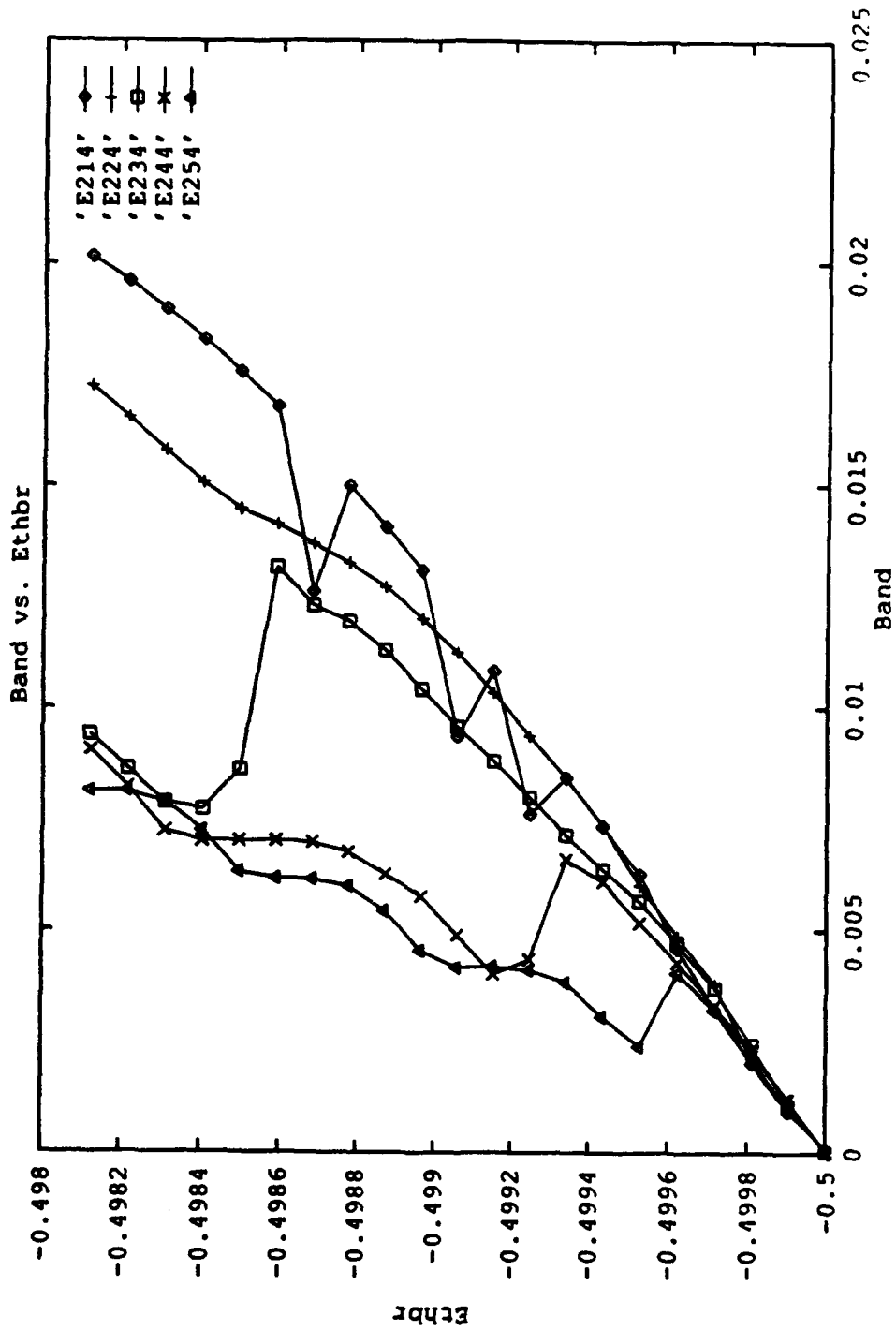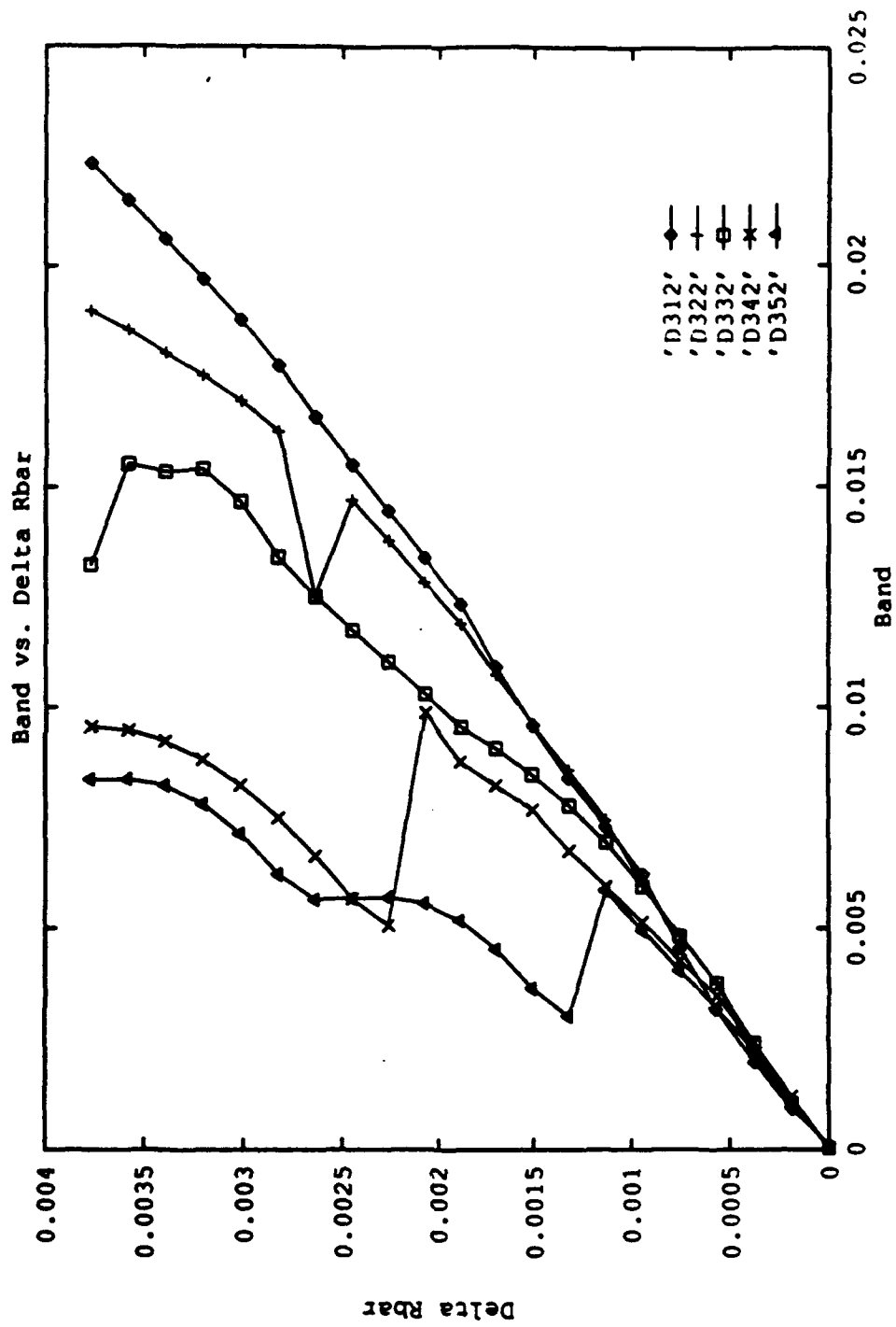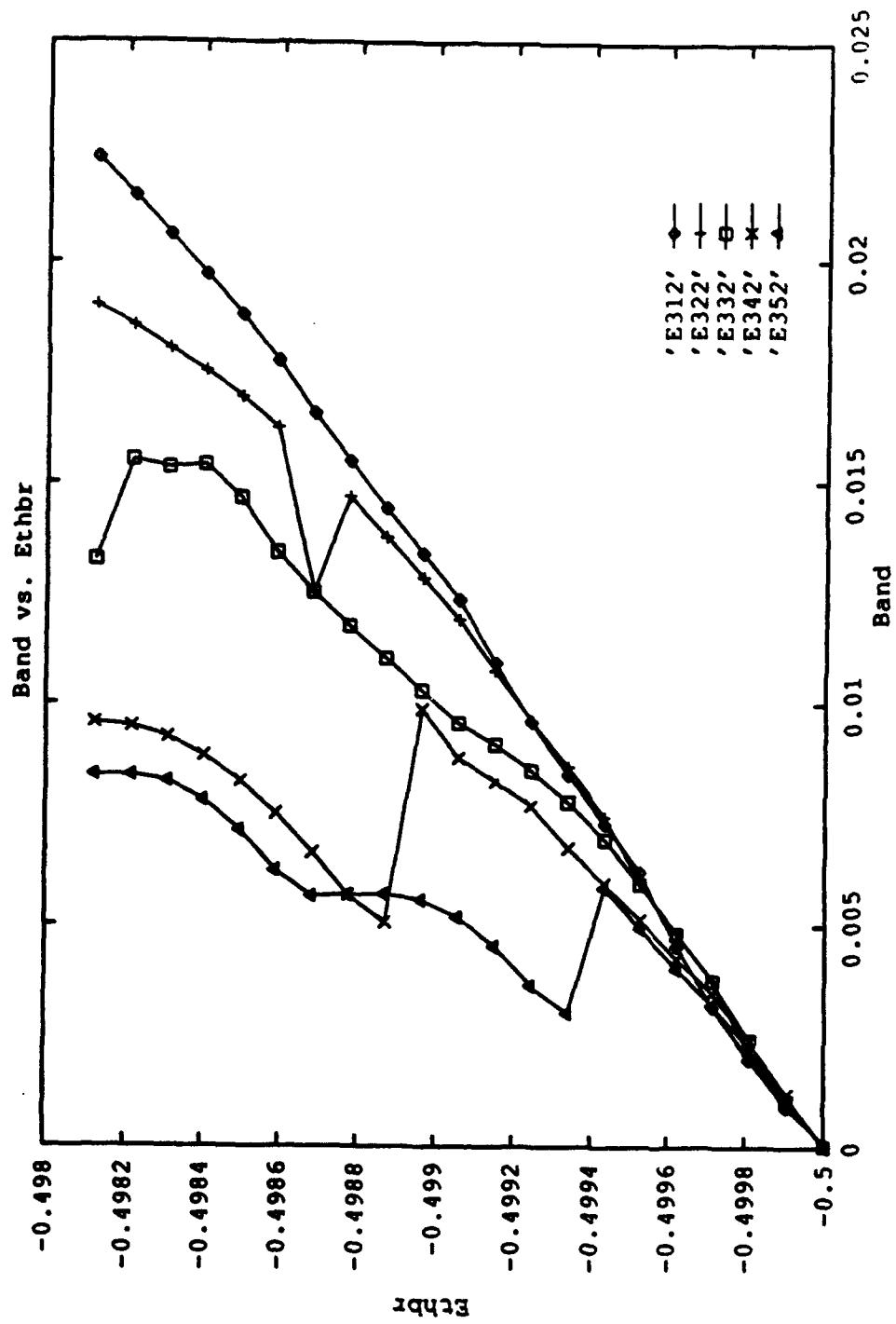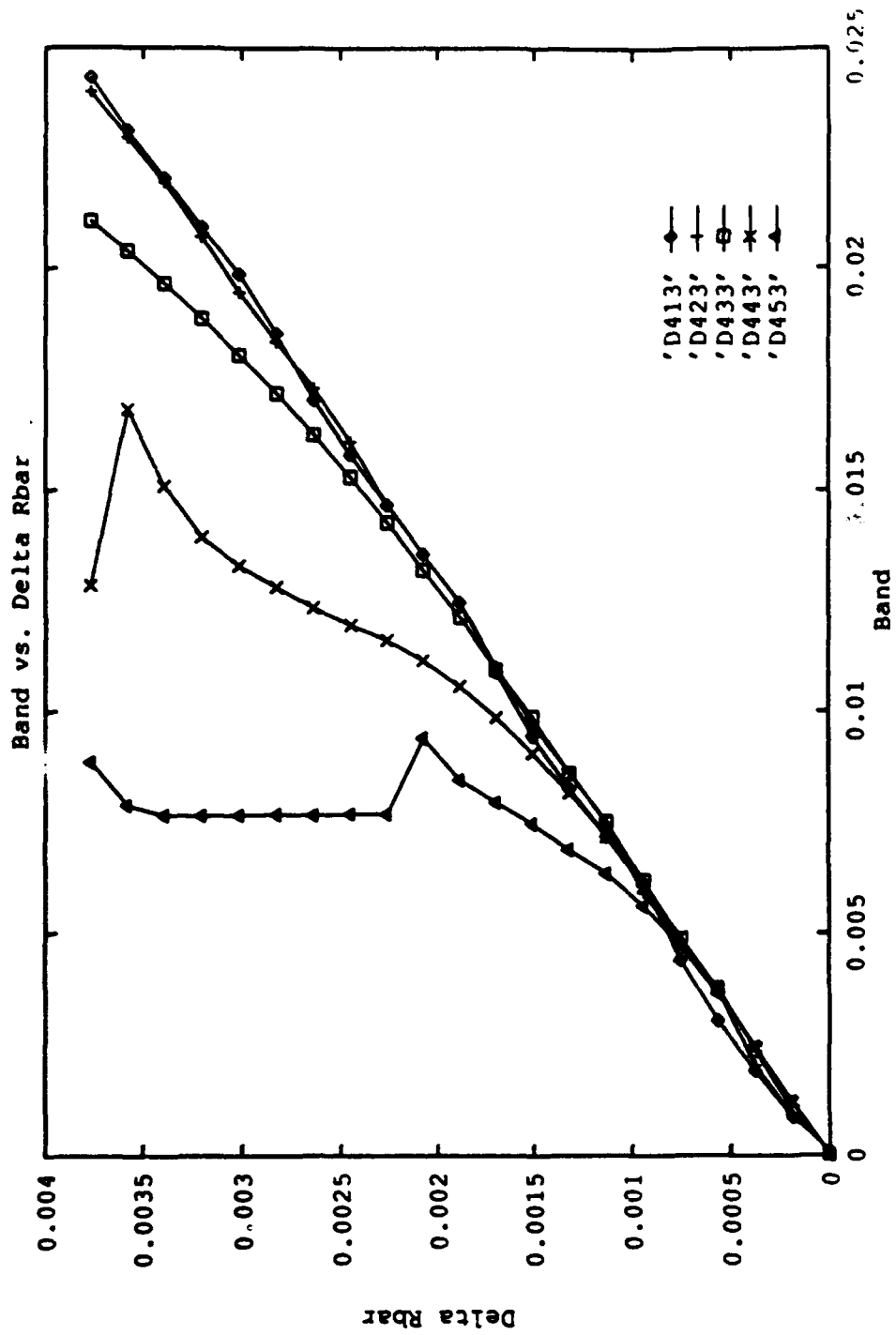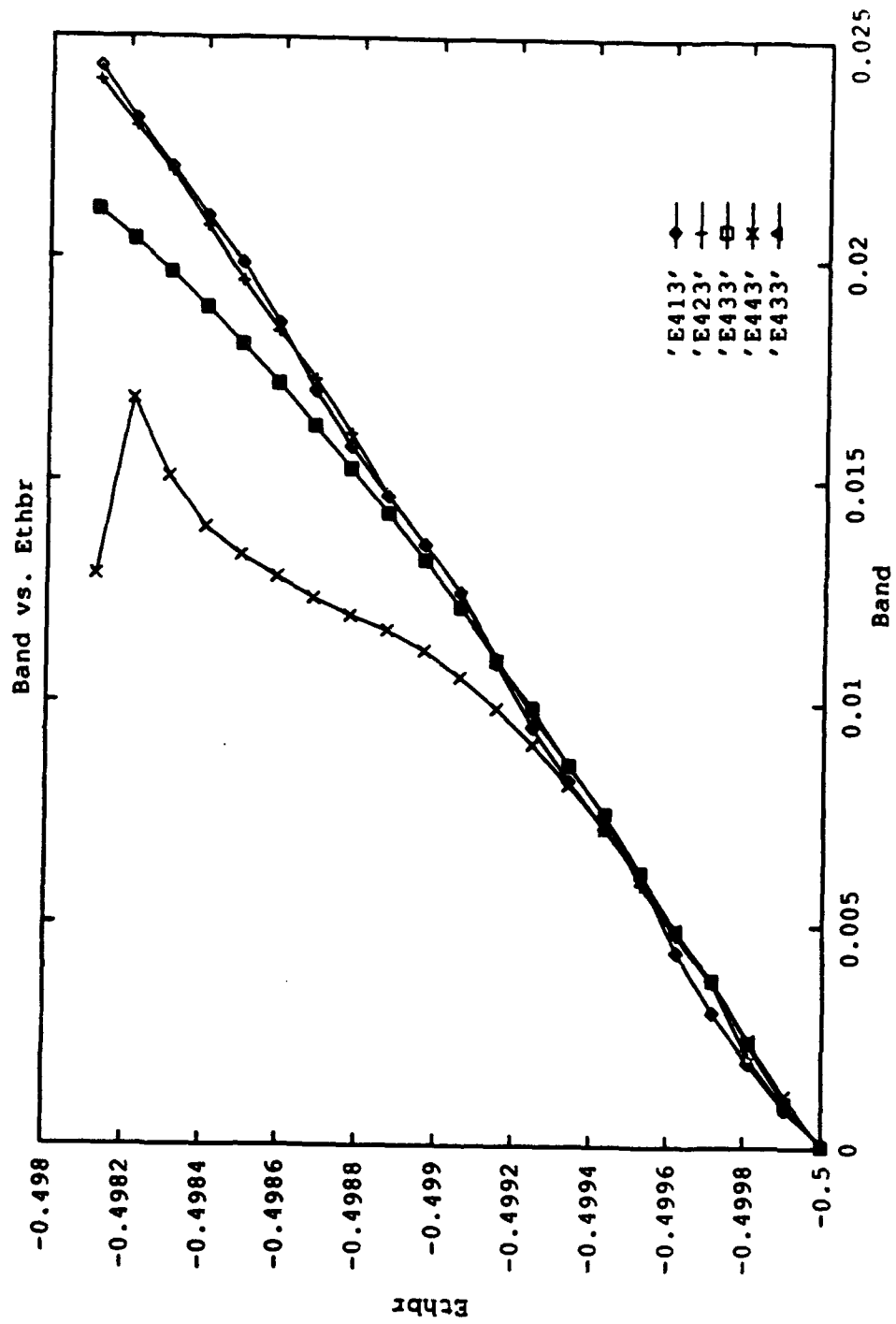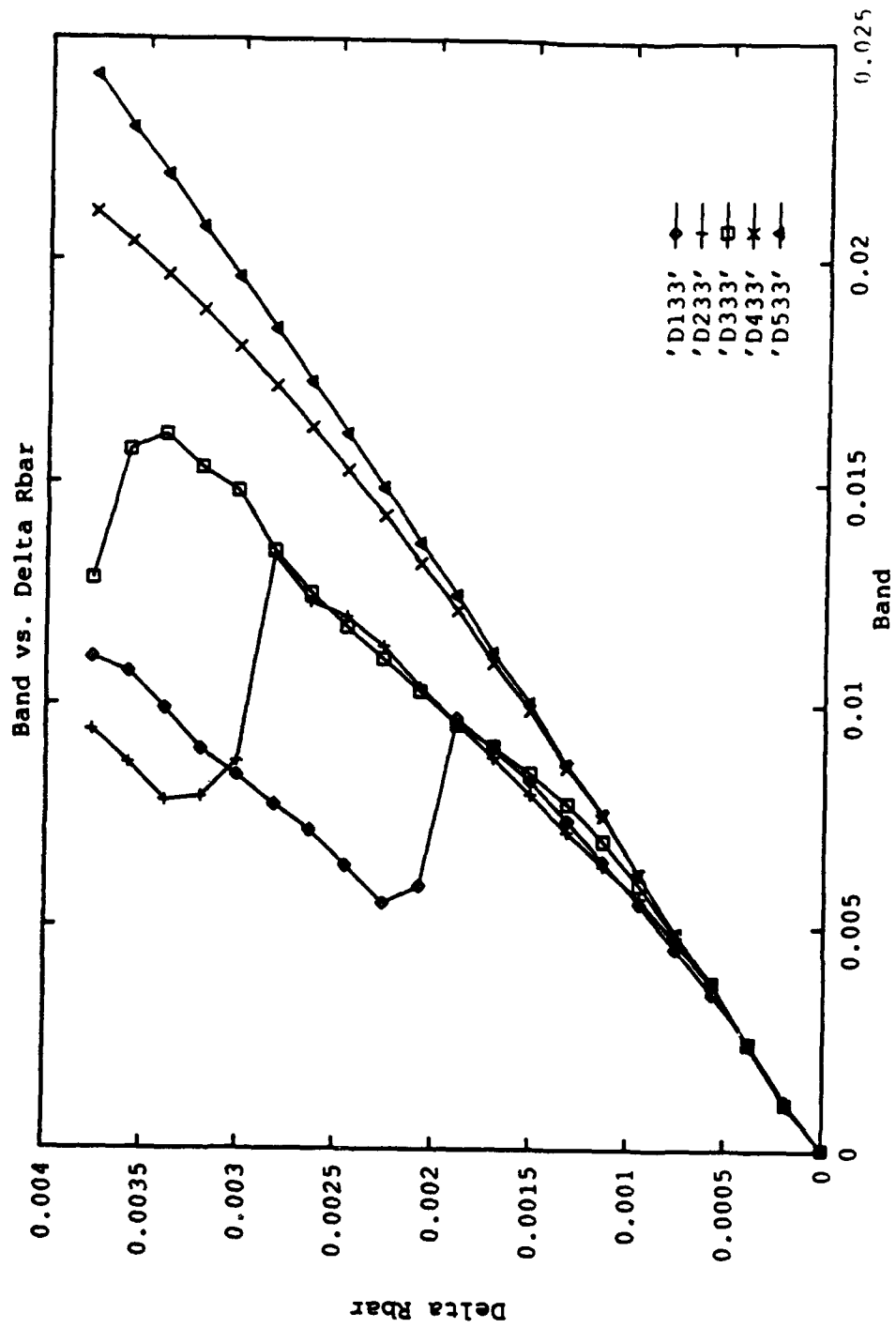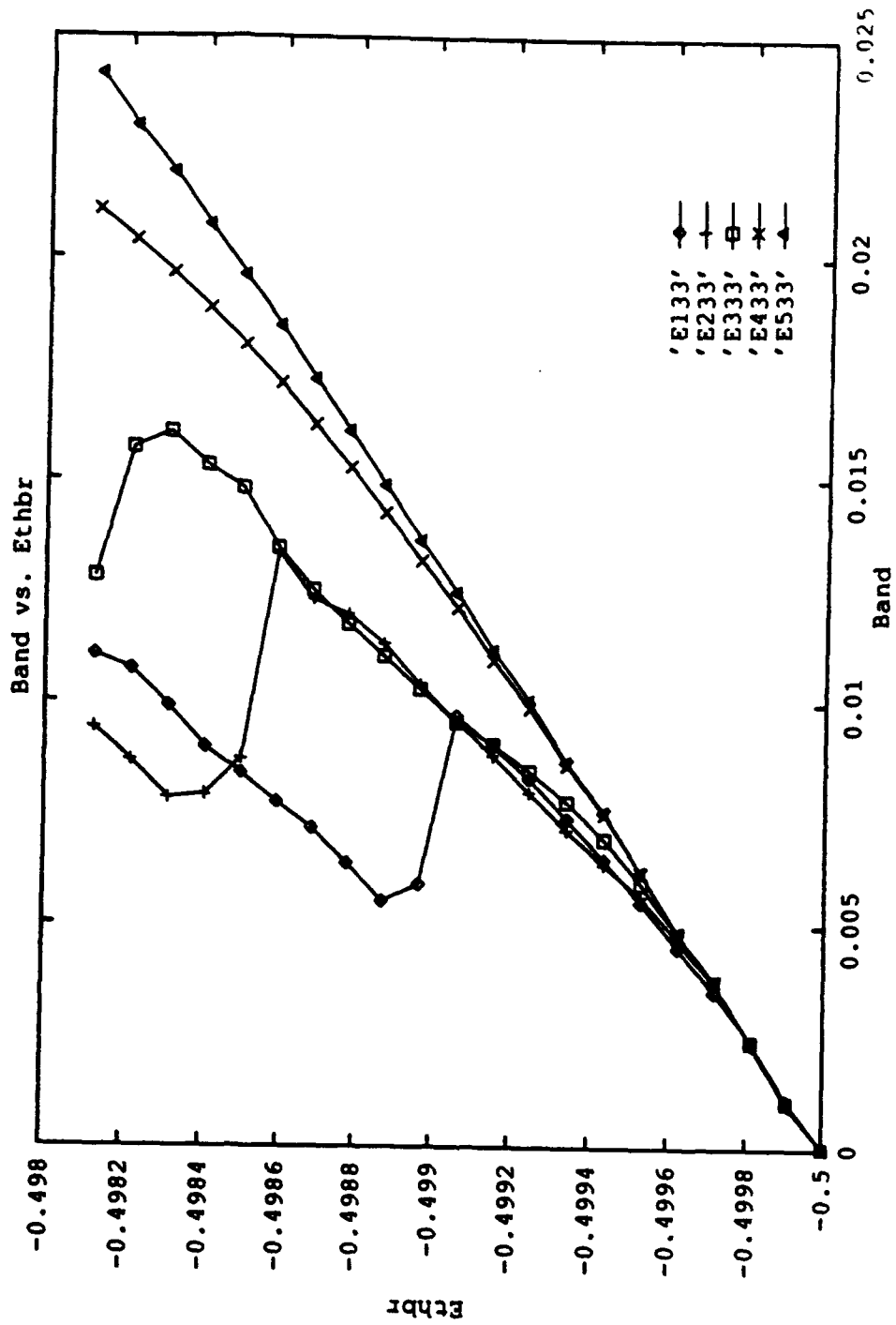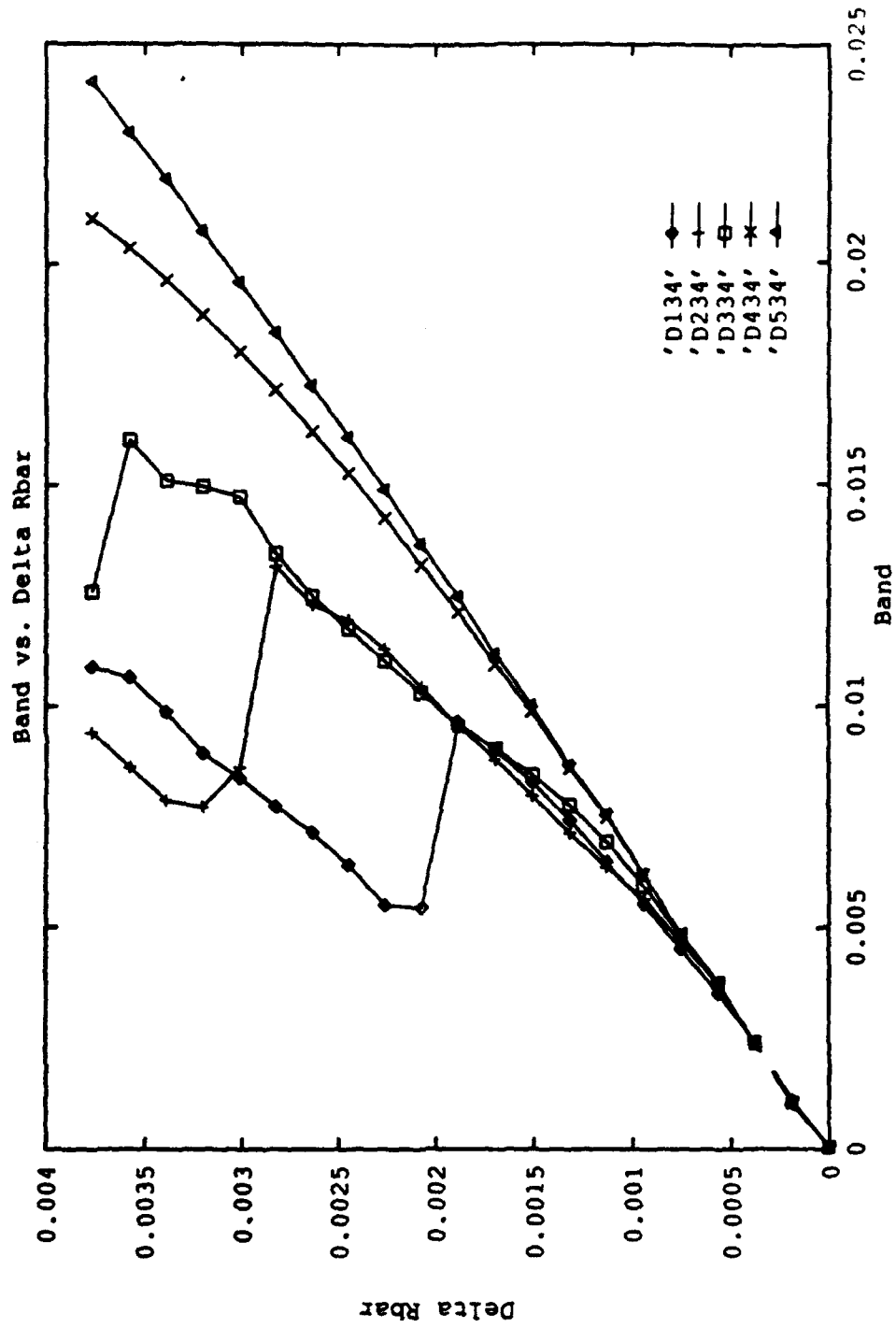
Band vs. Delta Rbar

Figure 12a

66

Figure 12b

67

Figure 13a

68

Figure 13b

69

Figure 14

70
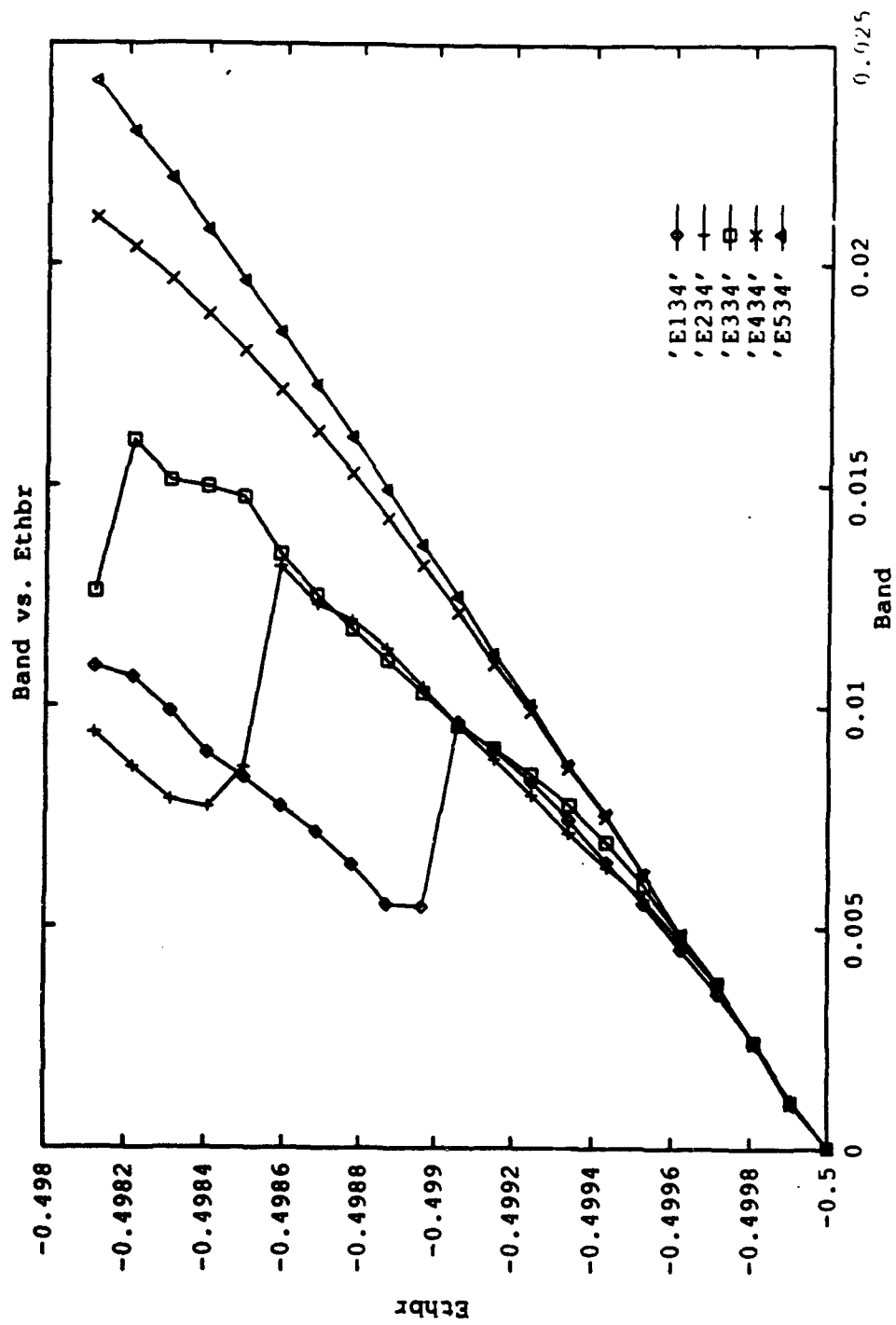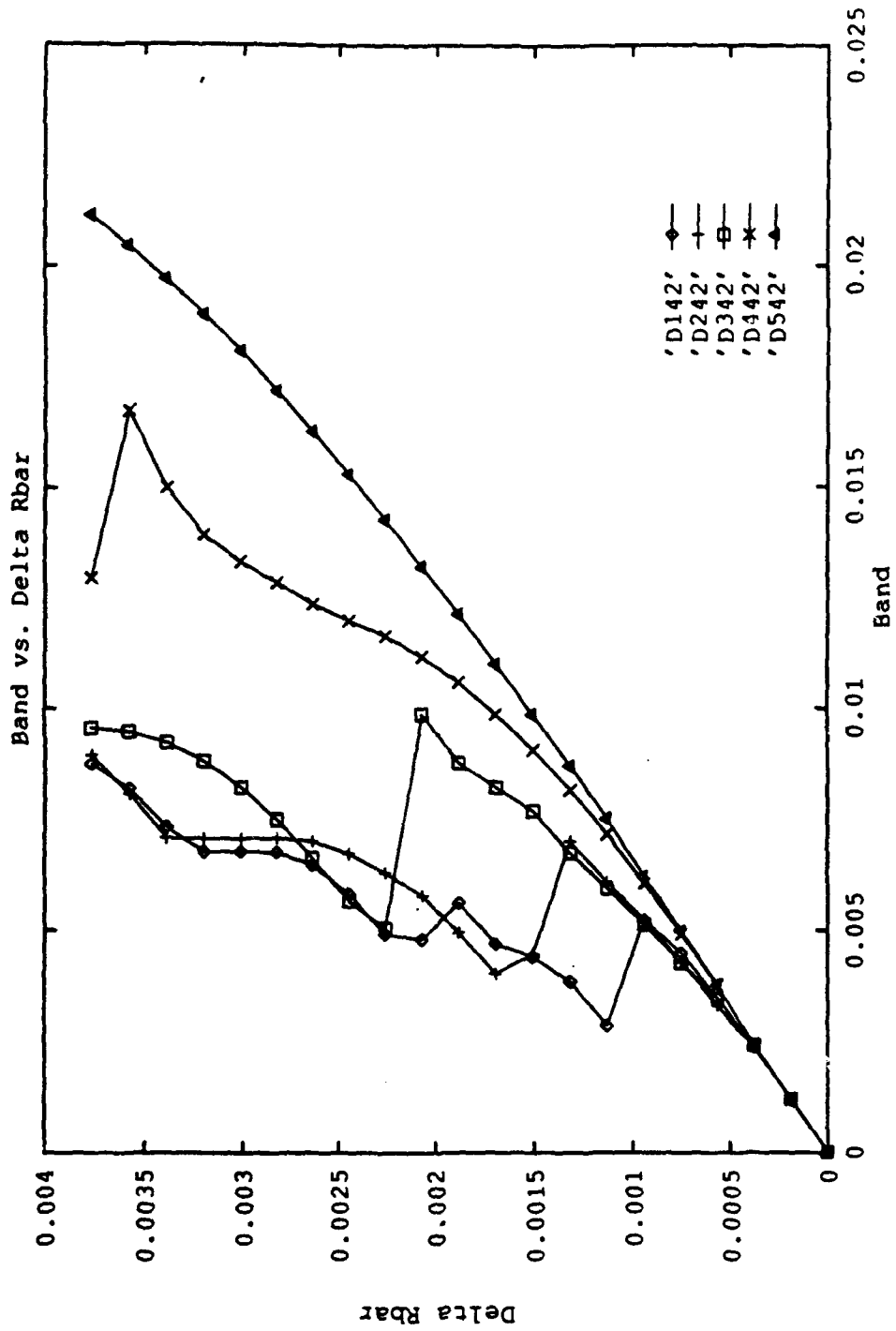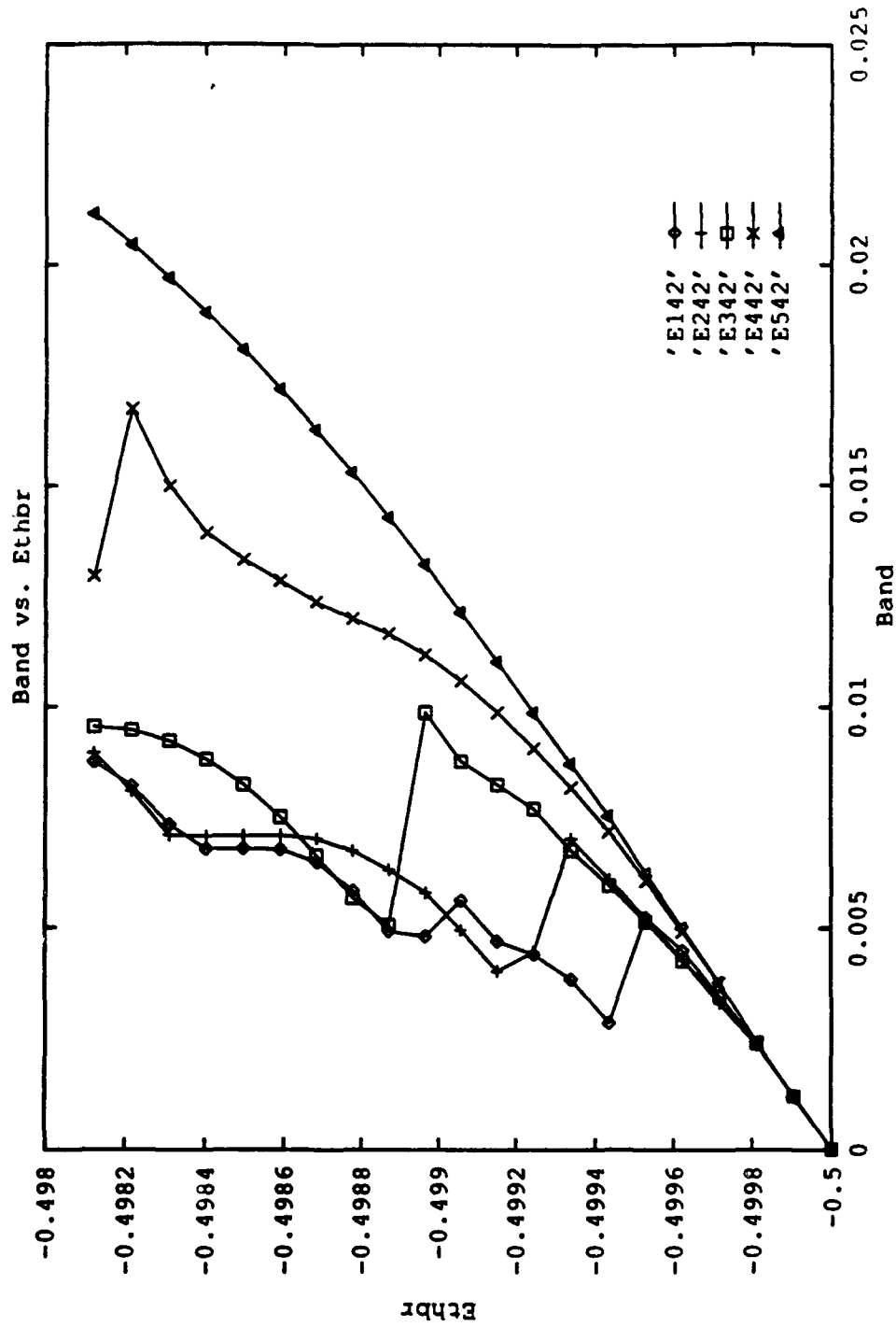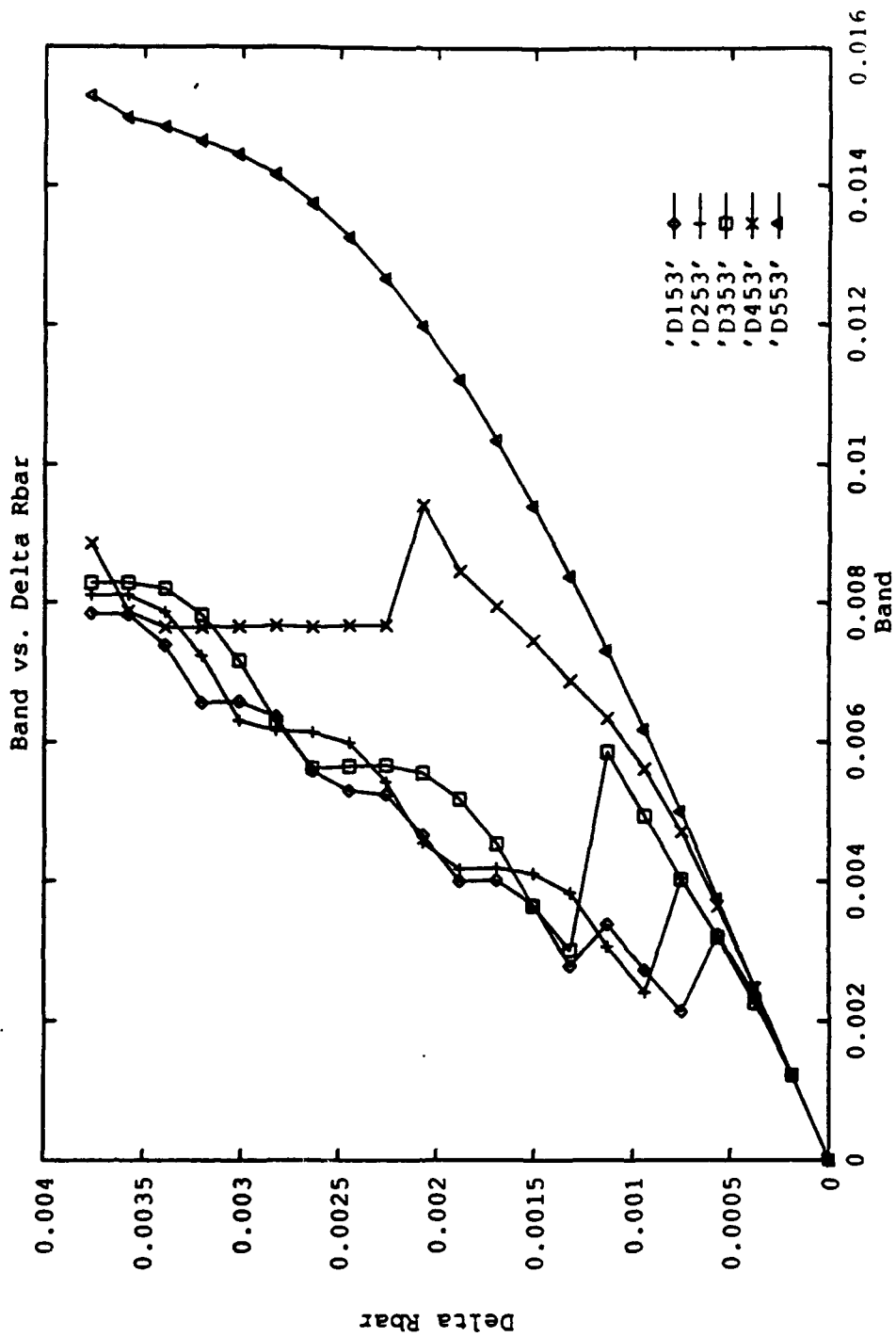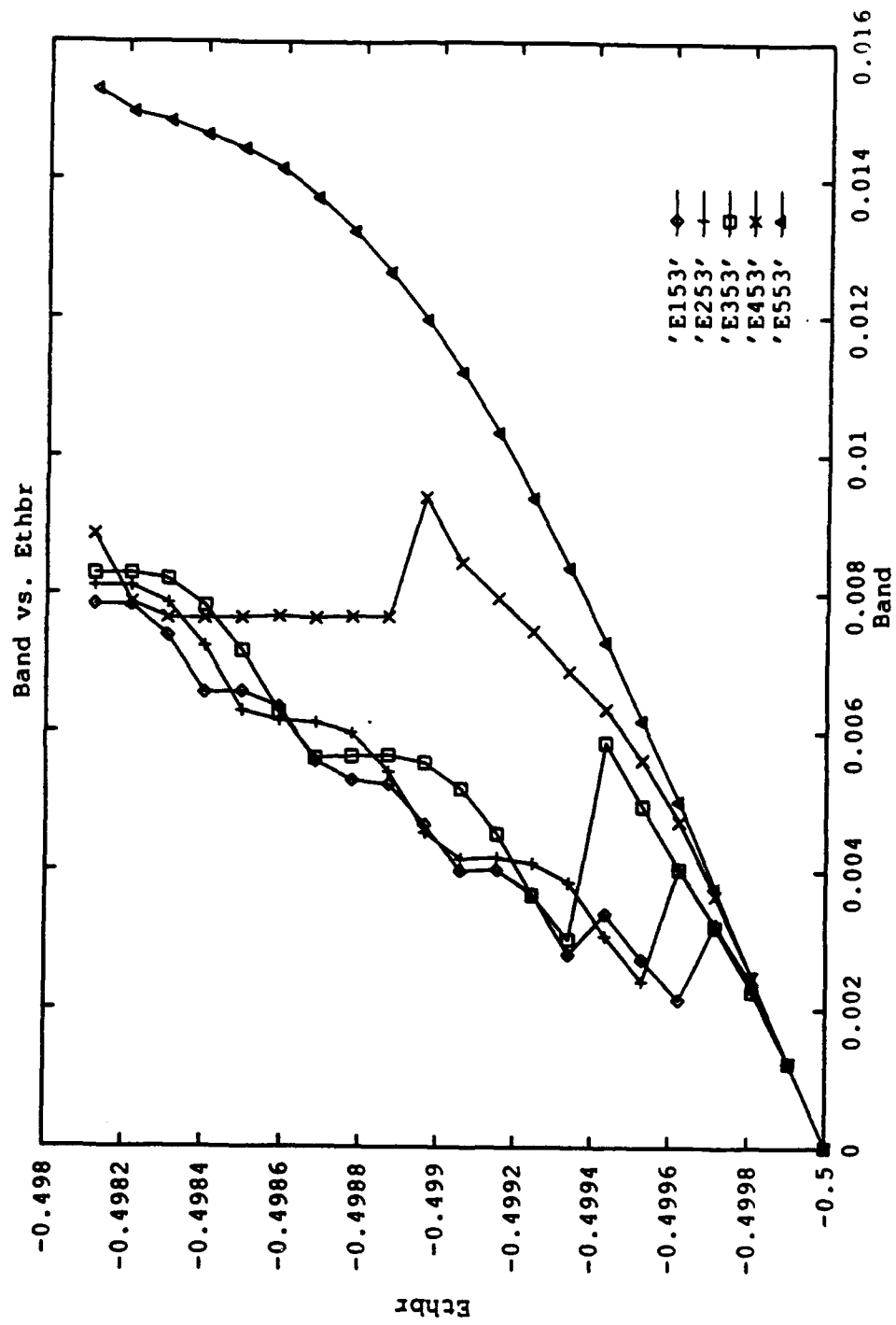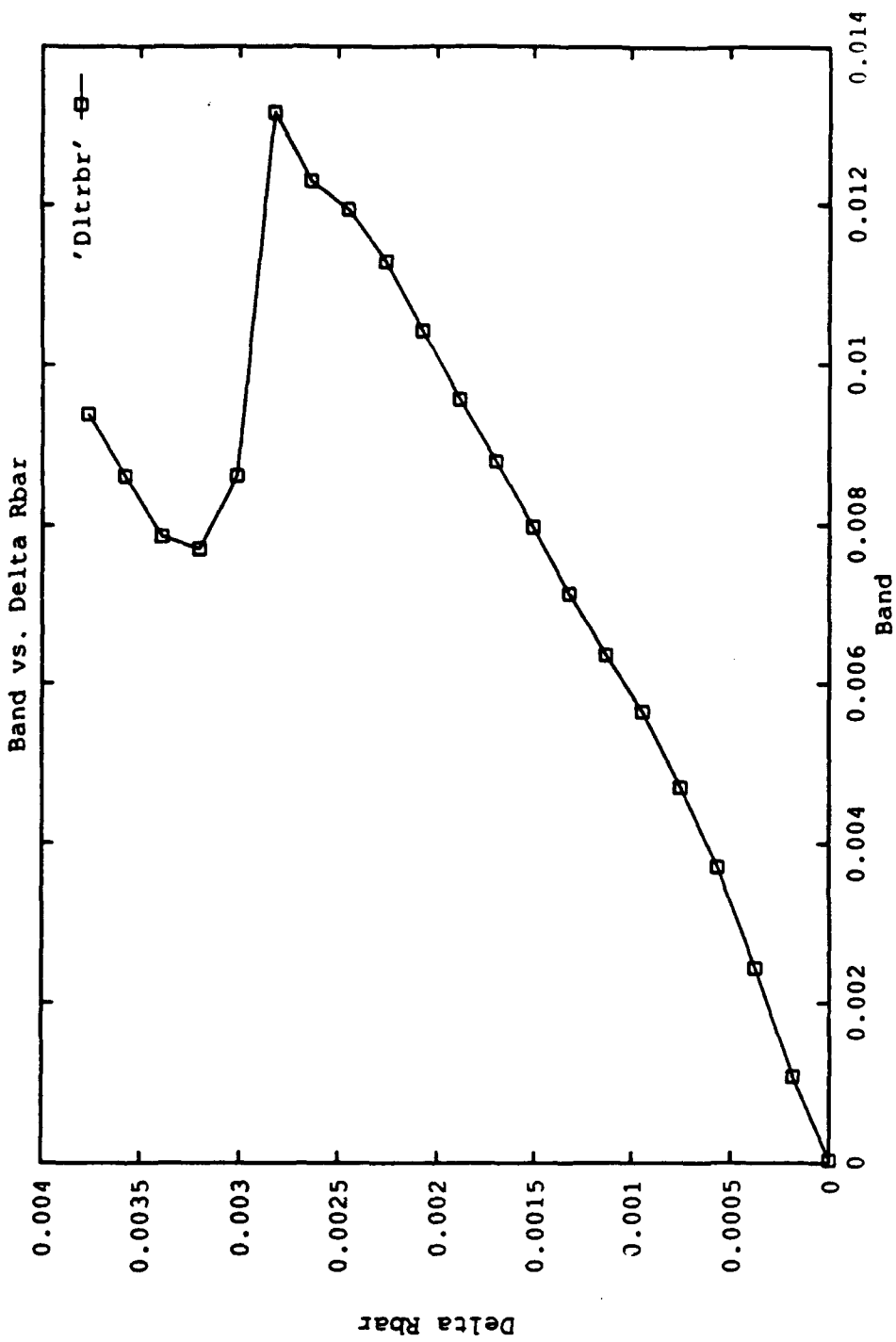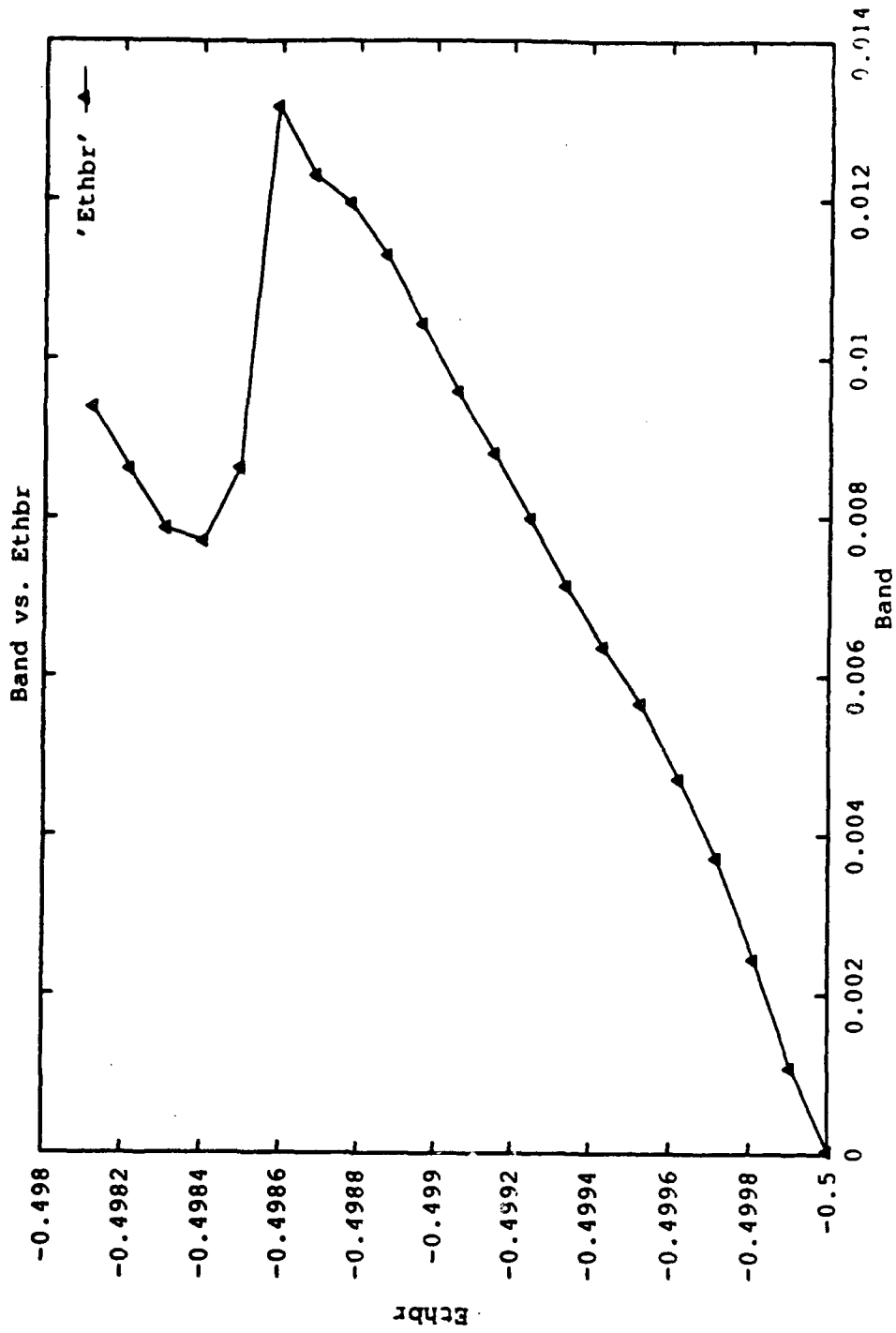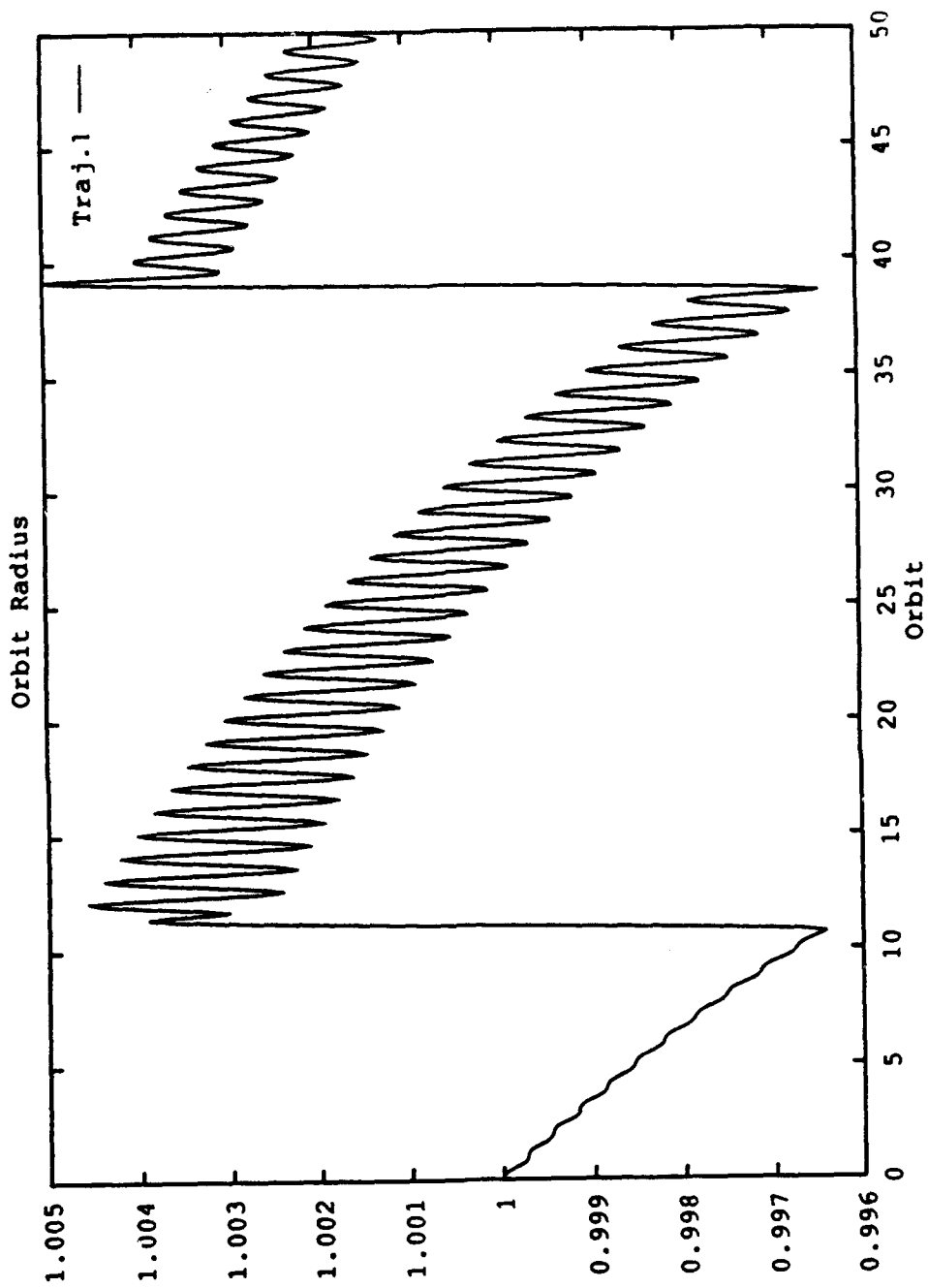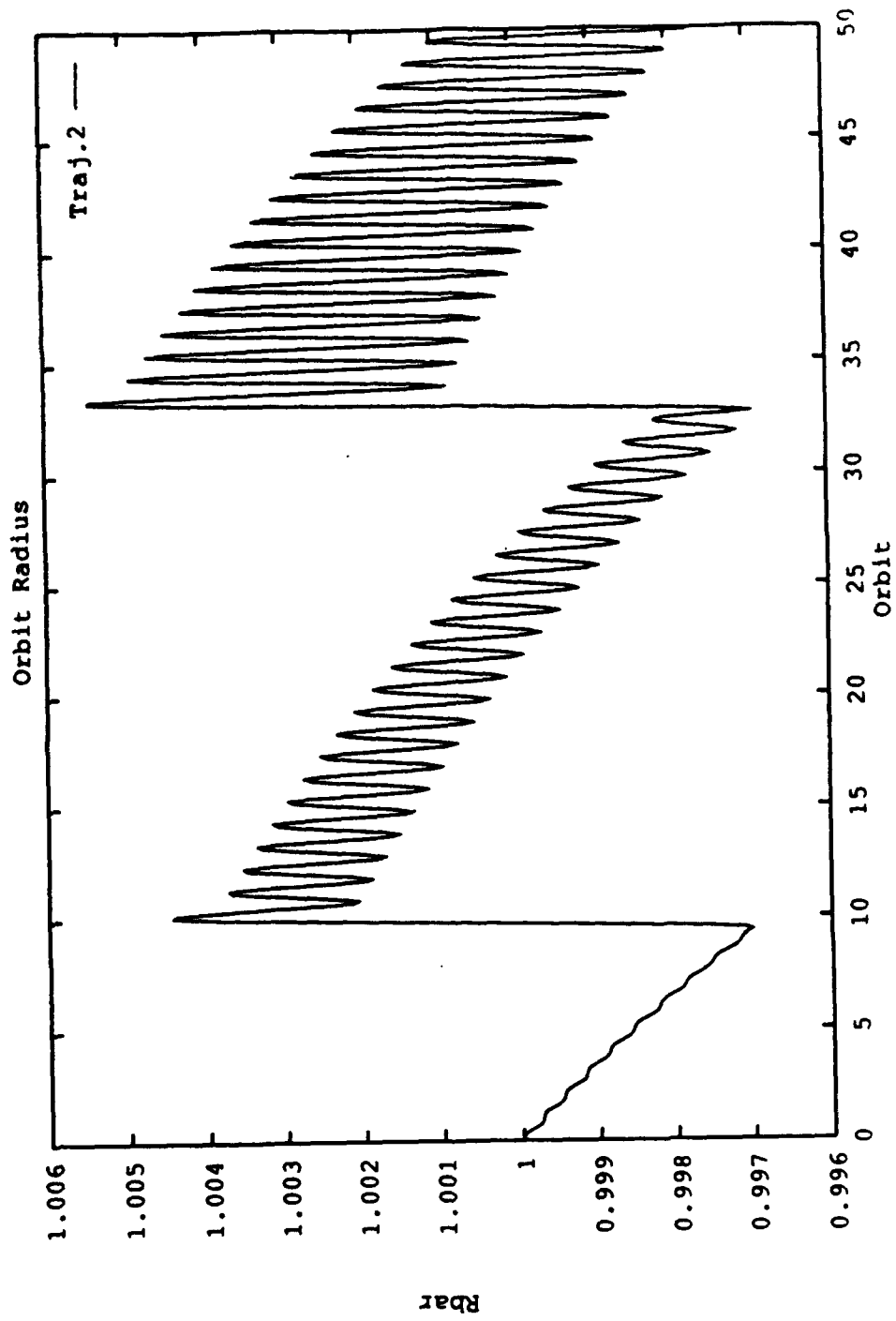
Figure 15

Figure 16

72

Figure 17

73

Figure 18

74

Figure 19

75

Figure 20

76

Figure 21

77
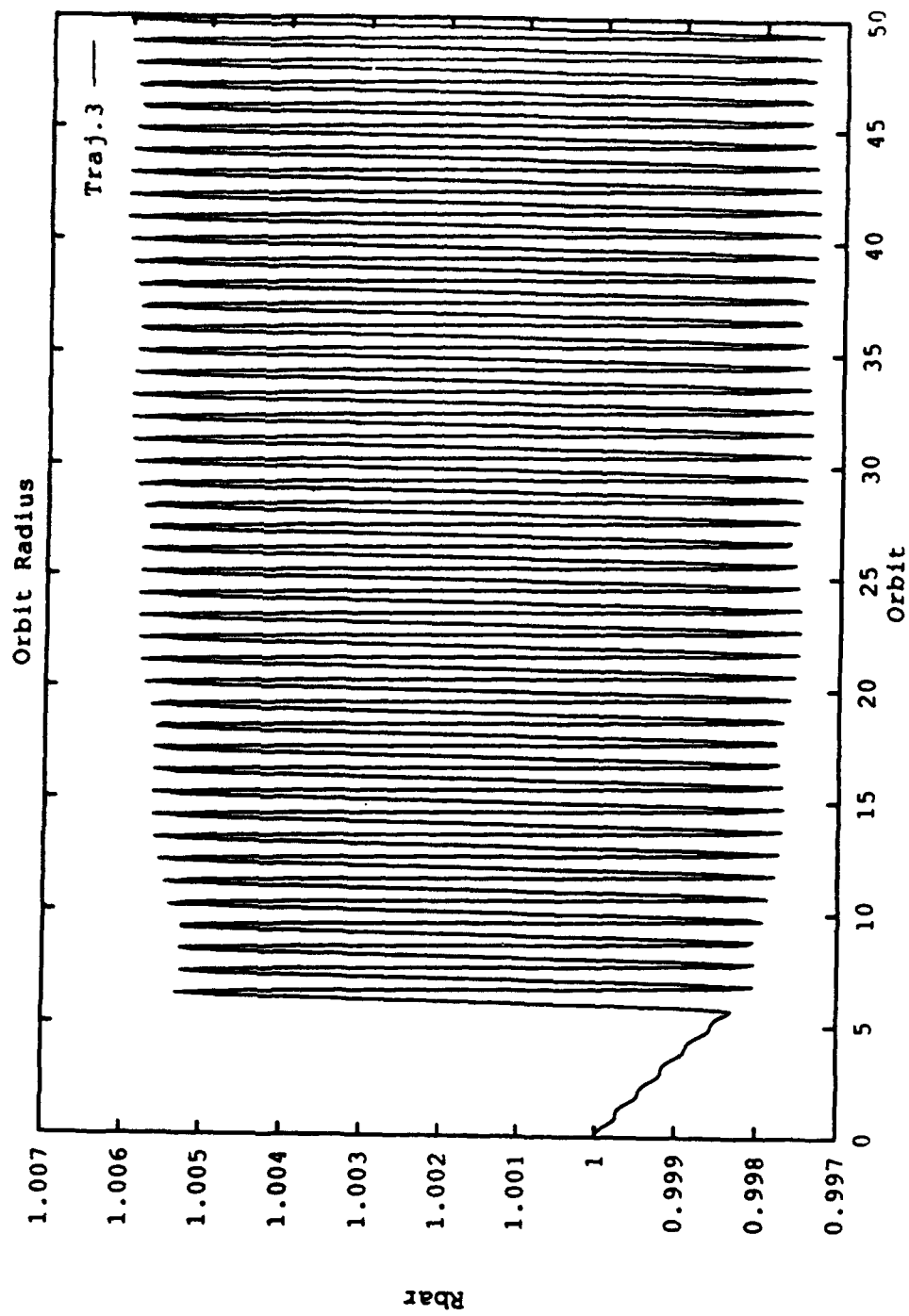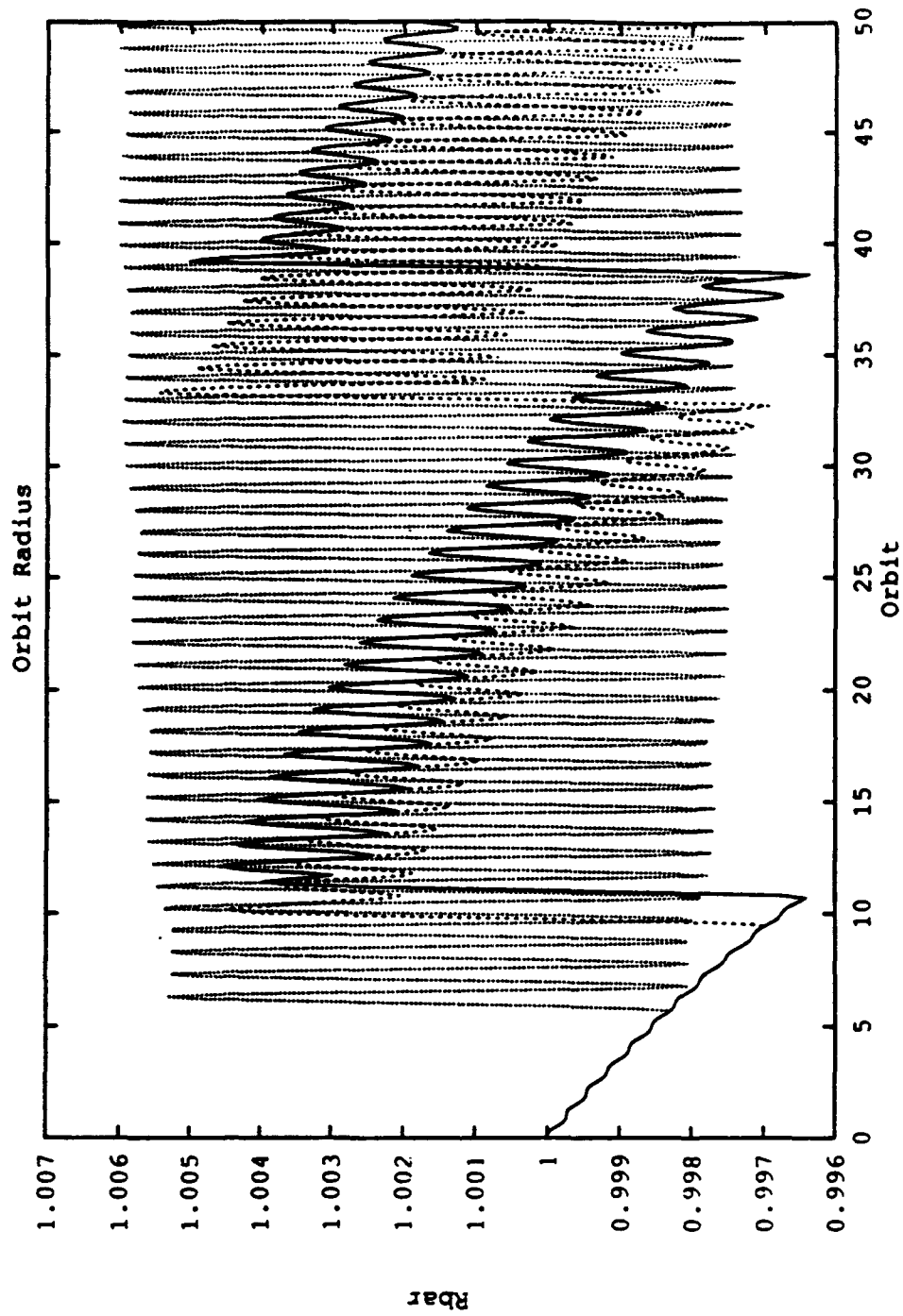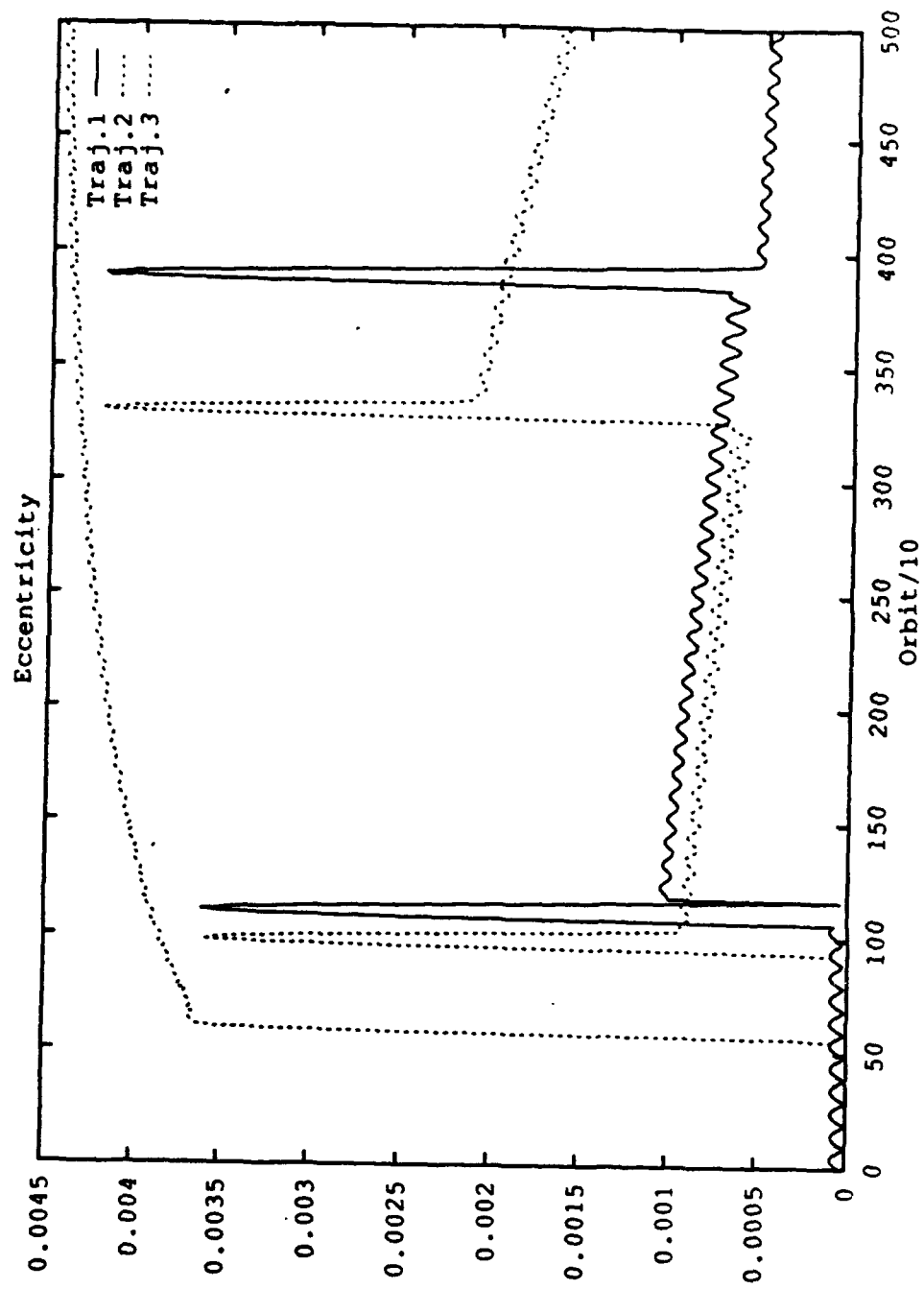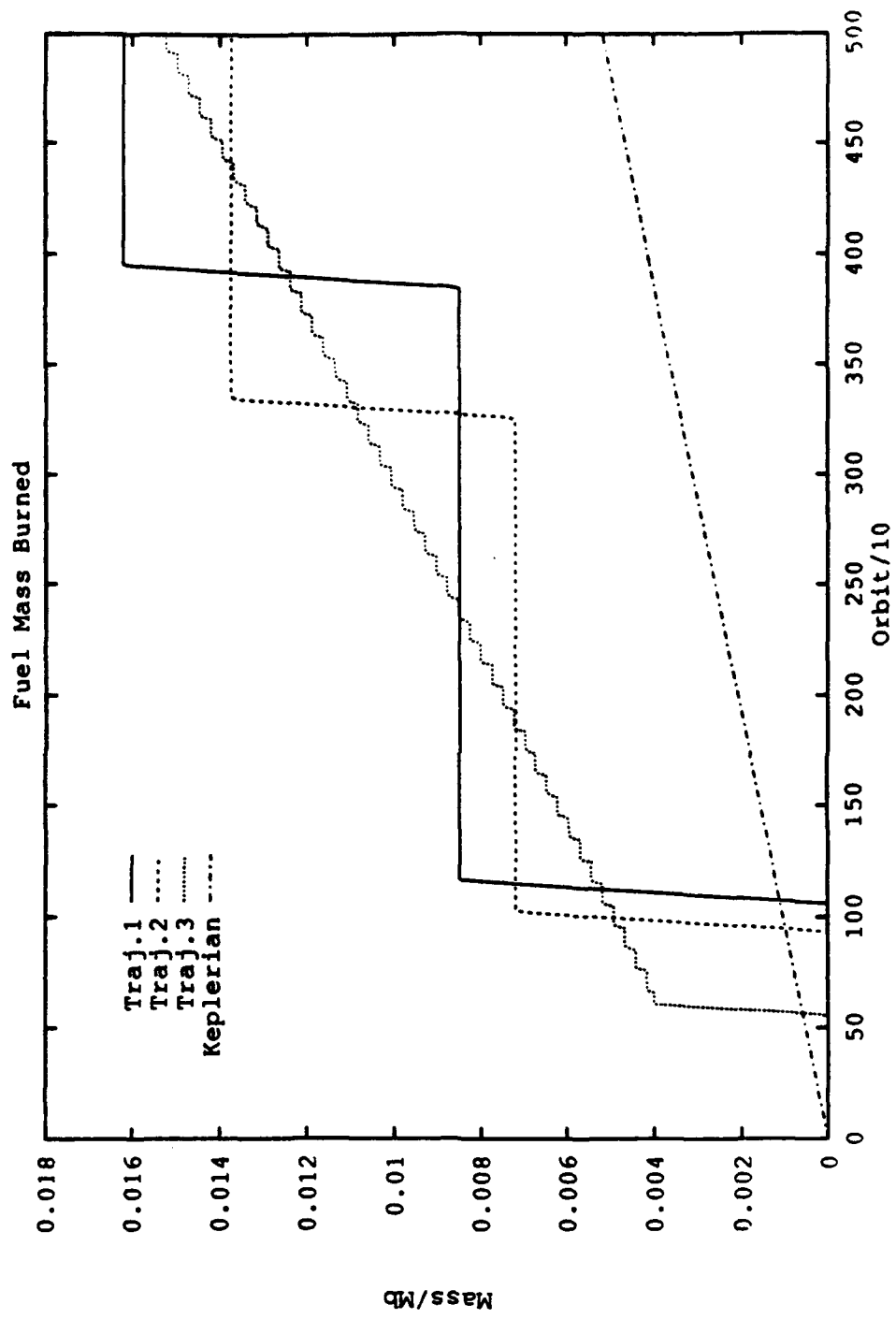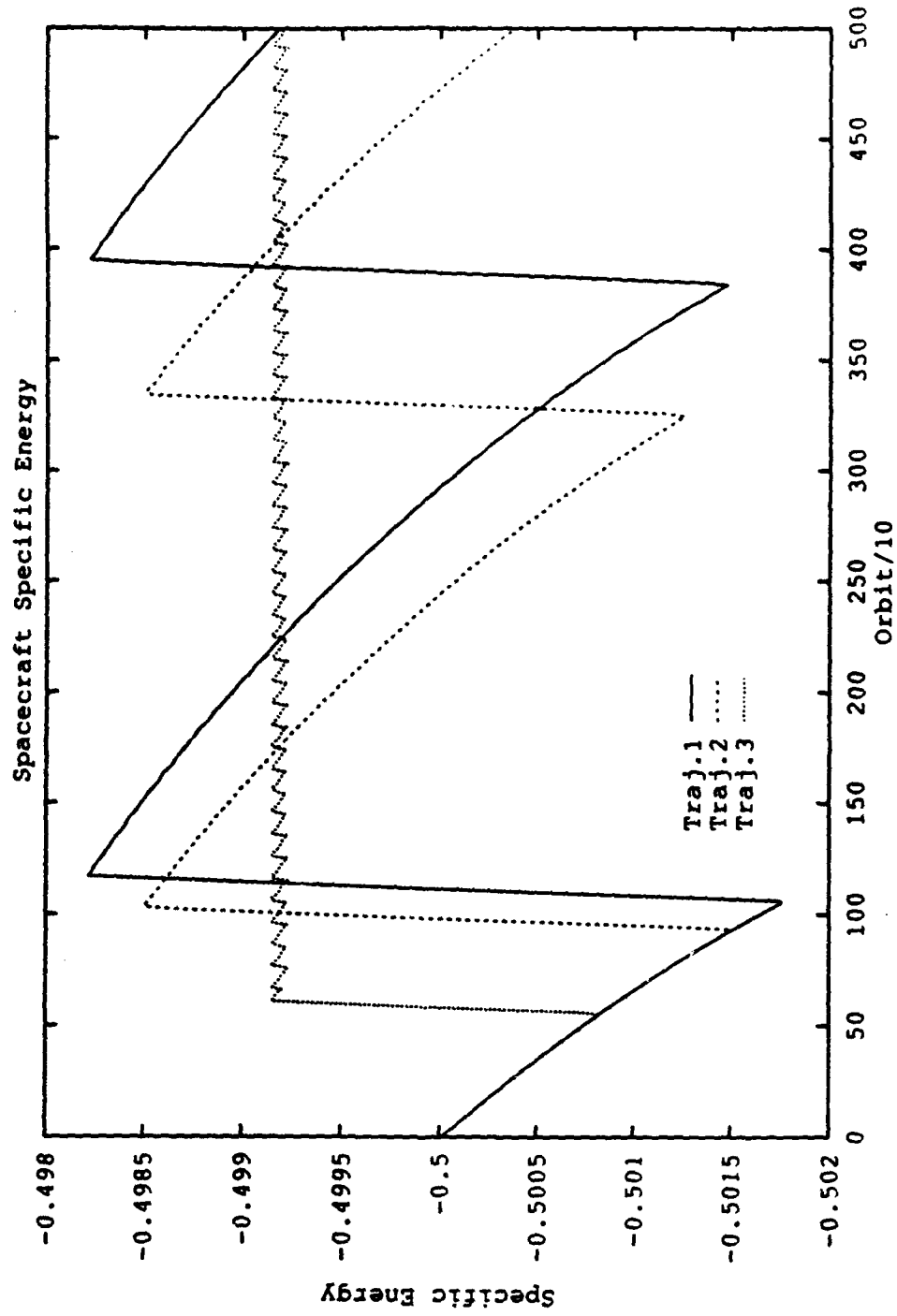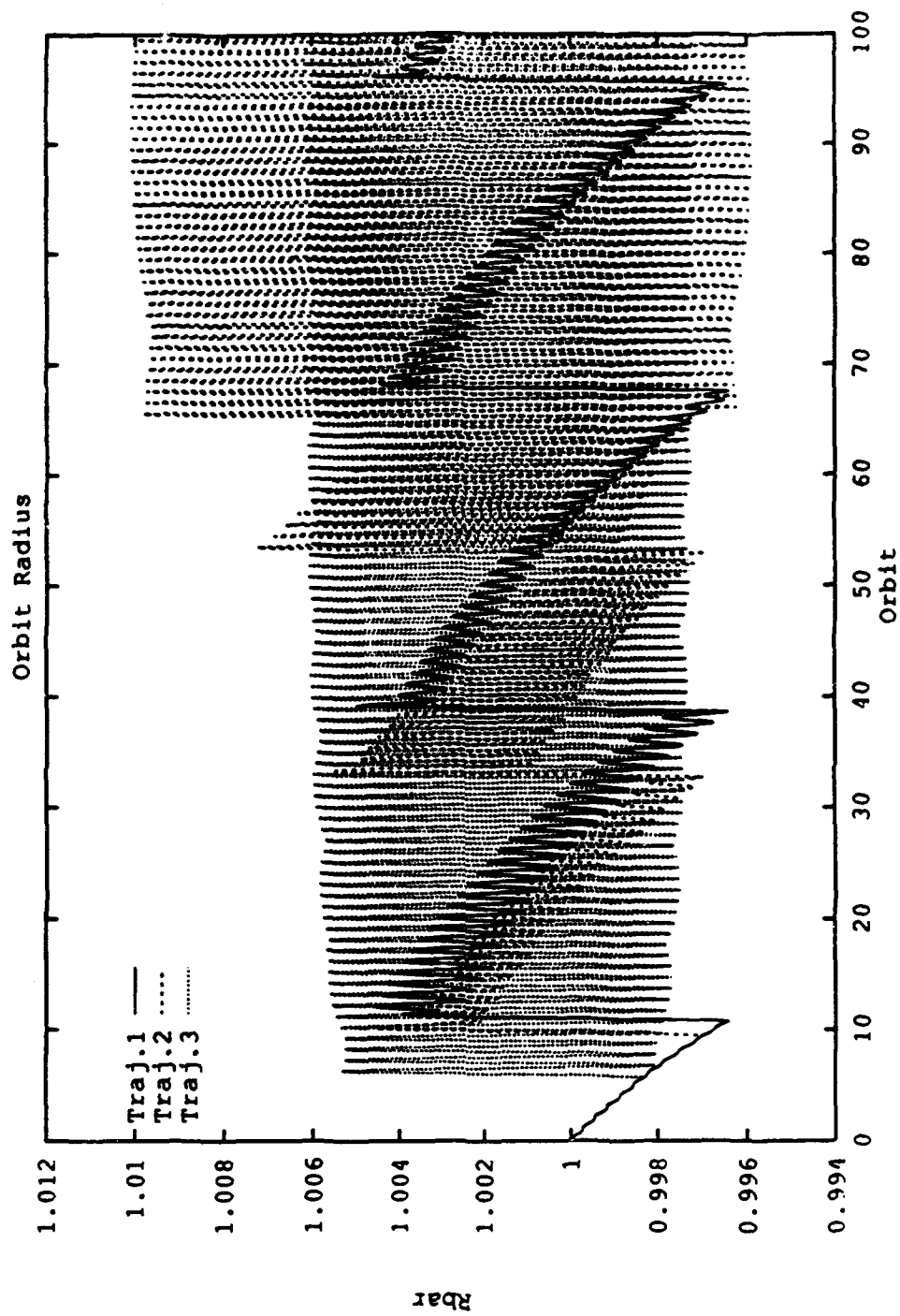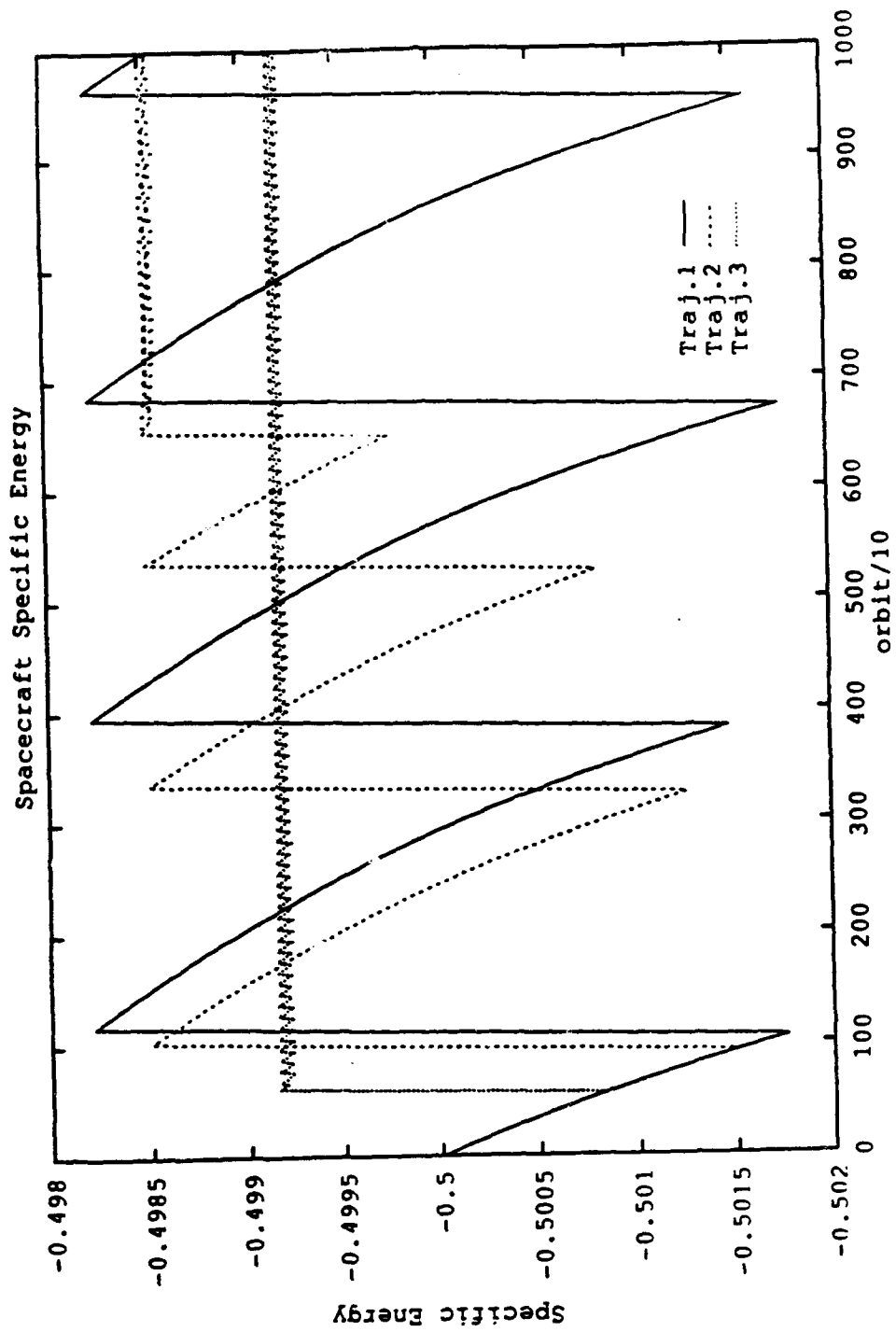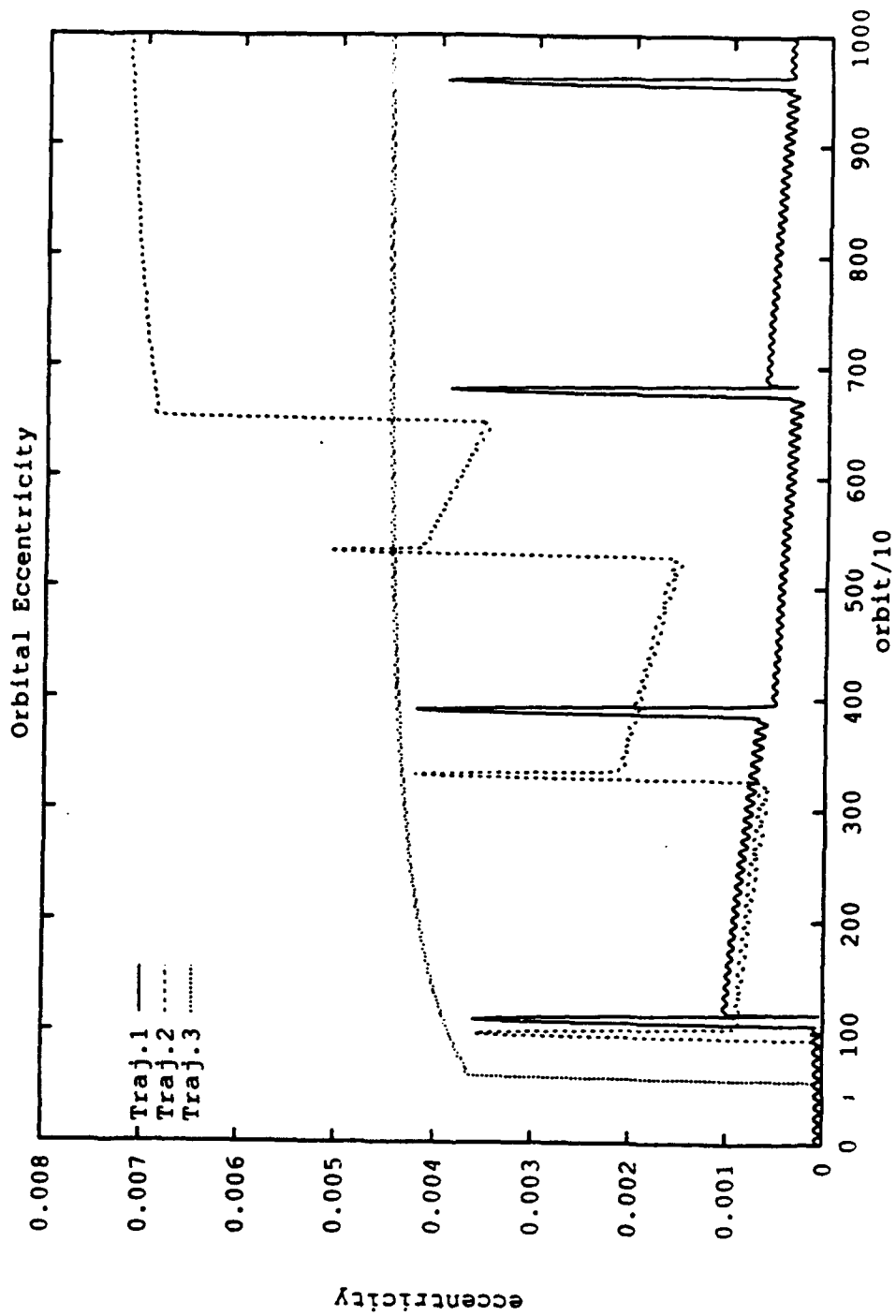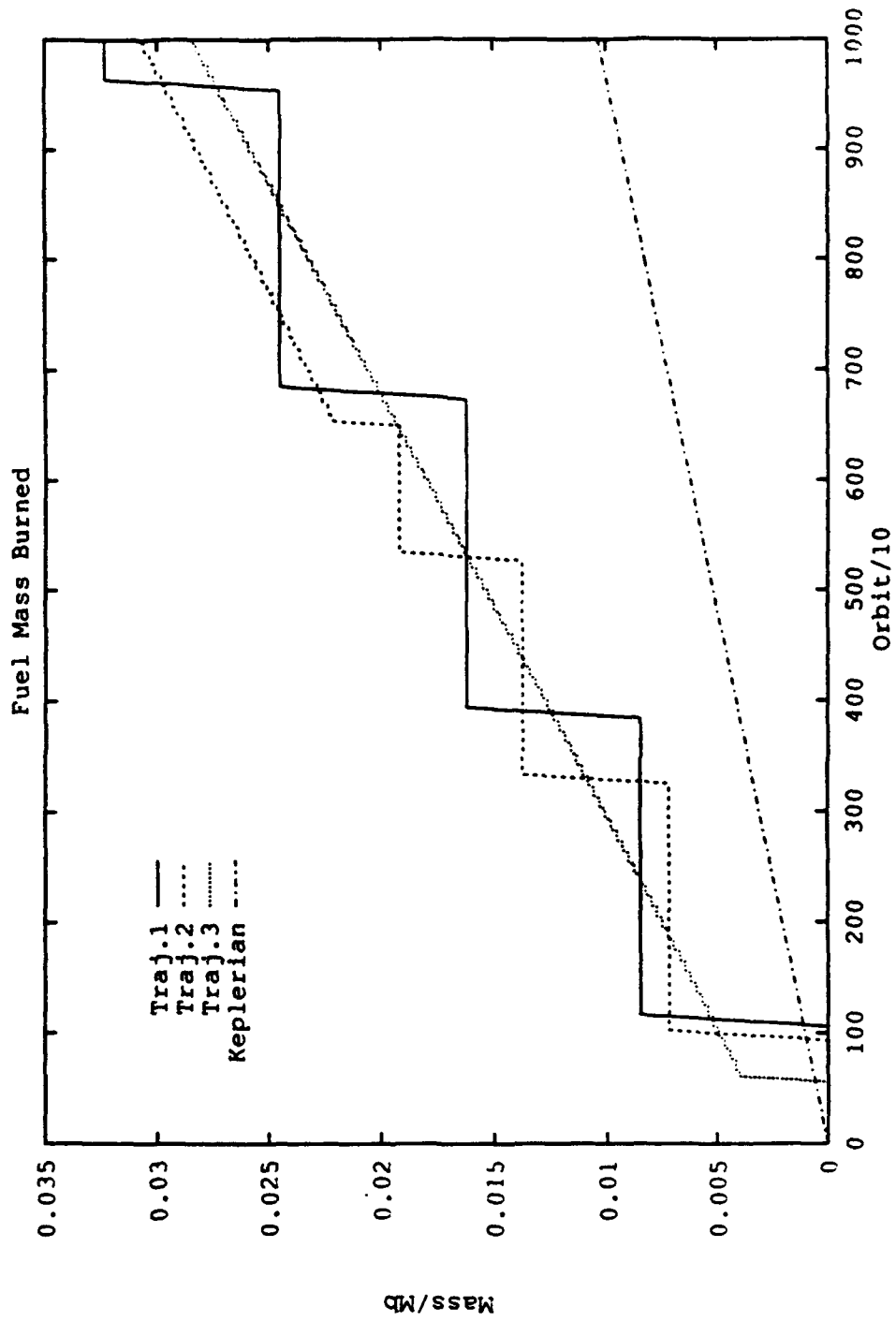
Figure 22

Figure 23

Figure 24

LIST OF REFERENCES

1. Ross, I.M., and Melton, R.G., "Singular Arcs for a Blunt Endoatmospheric Vehicle," *The Journal of the Astronautical Sciences*, Vol. 41, No. 1, pp.35-51, January-March 1993

2. Gottlieb, R.G., "Eccentricity-Intercept Targeting and Guidance (EITAG)," paper presented at the GN&C Technical Exchange meeting 27 July 1989.

3. Pauls, D.D., *Orbital Maintenance of Endoatmospheric Low Earth-Orbiting Satellites*, Master's Thesis, Naval Postgraduate School, Monterey, California, December 1991.

4. Wilsey, M.S., *A Parametric Analysis of Endoatmospheric Low-Earth-Orbit Maintenance*, Master's Thesis, Naval Postgraduate School, Monterey, California, March 1993.

5. AA4850 Class Notes, Naval Postgraduate School, Monterey, California, Spring 1994.

6. Ross, I.M., Pauls, D.D., and Wilsey, M.S., "Utility of Forced Keplerian Trajectories in Low-Earth-Orbit Maintenance," AAS paper 94-111, presented at the AAS/AIAA Spaceflight Mechanics Meeting, Cocoa Beach, Florida, February 14-16, 1994.

INITIAL DISTRIBUTION LIST

1. Defense Technical Information Center   2
   Cameron Station
   Alexandria, Virginia 22304-6145

2. Library, Code 52   2
   Naval Postgraduate School
   Monterey, California 93943-5101

3. I. M. Ross, Code AA/Ro   9
   Naval Postgraduate School
   Monterey, California 93943-5000

4. S. Scrivener, Code AA/Sc   1
   Naval Postgraduate School
   Monterey, California 93943-5000

5. Paul A. Gardner   1
   1144 Ocean View Dr.
   Anchorage, Alaska 99515